# Five Possible Isocyanoazulenes and Electron-Rich Complexes Thereof: A Quantitative Organometallic Approach for Probing Electronic Inhomogeneity of the Azulenic Framework

Randall E. Robinson, Thomas C. Holovics, Stephan F. Deplazes, Douglas R. Powell, Gerald H. Lushington, Ward H. Thompson, and Mikhail V. Barybin*

*Department of Chemistry, The University of Kansas, 1251 Wescoe Hall Drive, Lawrence, Kansas 66045*

*Received March 21, 2005*

Efficient syntheses of all five possible isocyanoazulenes, the four isomeric archetypal compounds $CN^1Az$, $CN^2Az$, $CN^4Az$, and $CN^6Az$, as well as the 1,3-di-*tert*-butyl derivative of $CN^5Az$ (Az = azulenyl), are described. Compounds $CN^1Az$ and $CN^2Az$ show unexpected shifts of the $S_0 \rightarrow S_1$ transition in their electronic spectra relative to azulene. The origins of these "anomalous" shifts have been addressed by DFT calculations, cyclic voltammetry, and comparison of the electronic spectra of isocyanoazulenes with those of the corresponding isomeric cyanoazulenes. Despite the high propensity of the azulenic nucleus to undergo multihapto coordination and C−C coupling in the presence of low-valent metals, the isocyanoazulenes react with $^1/_6$ equiv of Cr($\eta^6$-naphthalene)$_2$ to afford thermally stable Cr(CN$^x$Az)$_6$ ($x$ = 1, 2, 4, 6), which contain six discrete azulenyl groups separated from the Cr center by isocyanide linkers. All Cr(CN$^x$Az)$_6$ species undergo oxidation to form the corresponding paramagnetic cations [Cr(CN$^x$Az)$_6$]$^+$, which have been crystallographically characterized. Changing the atom of attachment of the azulenyl groups to the "Cr(CN)$_6$" core substantially alters the donor/acceptor properties of the isocyanoazulene ligands. The half-wave $Cr^{0/+}$ and $Cr^{+/2+}$ redox potentials for [Cr(CN$^x$Az)$_6$]$^z$ form the "electrochemical series" that constitutes a quantitative measure of electronic inhomogeneity of the azulenic framework. Unpaired spin delocalization within the azulenic moieties of [Cr(CN$^x$Az)$_6$]$^+$ has been observed by multinuclear NMR. The $Cr^I(d\pi) \rightarrow CN^xAz(p\pi^*)$ interaction has been shown to be an important contributor to the mechanism of unpaired electron delocalization in [Cr(CN$^x$Az)$_6$]$^+$.

## Introduction

Substances incorporating the bicyclo[5.3.0]decapentaene motif had been first isolated from essential oils in the middle of the 19th century, but their nonbenzenoid nature was not recognized until 1936.[1] The parent molecule, $C_{10}H_8$, referred to as azulene, is an azure blue hydrocarbon, which has a dipole moment of 1.08 D (Figure 1).[2] Until the pioneering synthetic work of Hafner and Nozoe in the late 1950s,[3,4] azulenic compounds had been extremely difficult to access. Nowadays, natural and synthetic derivatives of azulene find applications in synthesis,[5] medicine and pharmacology,[6] the cosmetics industry,[7] as well as in the design of advanced polymers,[8] optical materials,[9] and liquid crystals.[10] When benchmarked against those of benzenoid aromatics, the properties of azulenes appear unusual, if not bewildering.[3] This is due to the fact that the azulenic framework constitutes a more general type

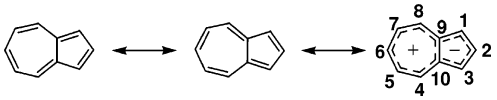


**Figure 1.** Azulene (bicyclo[5.3.0]decapentaene) and its atom-labeling scheme.

* To whom correspondence should be addressed. E-mail: mbarybin@ku.edu.

(1) (a) Hansen, H. J. *Chimia* **1997**, *51*, 147−159. (b) Hansen, H. J. *Chimia* **1996**, *50*, 489−496.

(2) Anderson, A. G.; Steckler, B. M. *J. Am. Chem. Soc.* **1959**, *81*, 4941−4946.

(3) (a) Heilbronner, E. In *Non-Benzenoid Aromatic Compounds*; Ginsburg, D., Ed.; Interscience Publishers: New York, 1959; pp 171−276. (b) Lloyd, D. *NonBenzenoid Conjugated Carbocyclic Compounds*; Elsevier: New York, pp 351−377 and references therein.

(4) Mochalin, V. B.; Porshnev, Y. N. *Russ. Chem. Rev. (Engl. Transl.)* **1977**, *46*, 530−547 and references therein.

(5) Selected examples: (a) Crombie, A. L.; Kane, J. L.; Shea, K. M.; Danheiser, R. L. *J. Org. Chem.* **2004**, *69*, 8652−8667. (b) Lash, T. D.; Colby, D. A.; Graham, S. R.; Chaney, S. T. *J. Org. Chem.* **2004**, *69*, 8851−8864. (c) Ito, S.; Okujuma, T.; Kabuto, C.; Morita, N. *Tetrahedron* **2003**, *59*, 4651−4659. (d) Lu, Y.; Lemal, D. M.; Jasinski, J. P. *J. Am. Chem. Soc.* **2000**, *122*, 2440−2445.

(6) Selected examples: (a) Rekka, E.; Chrysselis, M.; Siskou, I.; Kourounakis, A. *Chem. Pharm. Bull.* **2002**, *7*, 904−907. (b) Noguchi, K.; Kase, J.; Saitoh, M.; Masumiya, H.; Nakazawa, T.; Tanaka, Y.; Tanaka, H.; Hashimoto, K.; Shigenobu, K *Pharmacology* **2002**, *64*, 36−42. (c) Tanaka, Y.; Shigenobu, K. *Cardiovasc. Drug Rev.* **2001**, *19*, 297−312. (d) Asato, A. E.; Peng, A.; Hossain, M. Z.; Mirzadegan, T.; Bertram, J. S. *J. Med. Chem.* **1993**, *36*, 3137−3147.

(7) Bennett, S. In *Chemistry and Manufacture of Cosmetics*, 3rd ed.; Schlossman, M. L., Ed.; Allured: Carol Stream, IL, 2002; Vol. 3, p 243.

10.1021/om0502180 CCC: $30.25 
Publication on Web 04/15/2005

of aromaticity compared to the alternant systems, where $\pi$-electrons are dispersed *evenly* over *even*-membered rings. Despite great progress in understanding the physical and chemical consequences of electronic inhomogeneity of the azulenic scaffold,[5−10] the structure−property relationships in azulene chemistry remain somewhat fragile in terms of their generality,[5a] and some are being revisited.[11]

While the unusual physicochemical characteristics of azulene have led to the development of many advanced organic materials,[5−10] the use of the azulenic framework in designing functional organometallic systems has been far less explored.[9c,e,12] The majority of azulene-containing organometallics involve the azulenic nucleus coordinated to one or, more frequently, two or three metal centers in a multihapto (and, often, poorly predictable) fashion.[12c,13] The high tendency of azulene to engage in multihapto bonding, especially with low-valent metals, is nicely illustrated by the reaction of $Mo(\eta^6\text{-}C_6H_6)_2$ with azulene to give $(\eta^6\text{-}C_{10}H_8)Mo(\eta^6\text{-}C_6H_6)$, in which the azulenic moiety is coordinated to the Mo center via carbon atoms 1−4, 9, and 10.[13a] The metal-promoted C−C coupling of two azulene ligands is common,[13b,14] and the C−H activation of azulene by transition metals has been reported.[15] Species without direct interactions between a metal and the azulenic nucleus are rare and almost invariably involve metal ions bound to polydentate macrocycles (e.g., porphyrins)[12a,b] or "sandwiched" between $\eta^4$-cyclobutadienyl and/or $\eta^5$-cyclopentadienyl rings.[9c,e,16]

In 2003, we envisioned the class of azulene derivatives illustrated in Figure 2 and published a communication on the initial member of the isocyanoazulene family,

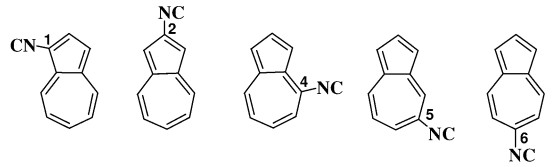


| | $CN^1Az$ | $CN^2Az$ | $CN^4Az$ | $CN^5Az$ | $CN^6Az$ |
|---|---|---|---|---|---|
| $p_e$ (D) | 4.99 | 5.40 | 3.82 | 3.77 | 3.14 |

**Figure 2.** Five possible isocyanoazulenes, $CN^xAz$ ($x$ denotes atom of attachment of the azulenyl group), and their calculated dipole moments, $p_e$, in the ground state.

6-isocyanoazulene ($CN^6Az$, Az = azulenyl).[17] Our interest in this type of compounds is associated with the design of hybrid metal-organic ensembles that do not possess direct metal−azulene bonds and feature the electronically ambivalent azulenic framework functioning as a donor, an acceptor, or a structural and electronic bridge. In this contribution, we demonstrate that azulenic moieties can be coupled to a low-valent metal center by means of isocyanide linkers and introduce the chemistry of all five possible isocyanoazulenes: the four isomeric "parent" compounds $CN^1Az$, $CN^2Az$, $CN^4Az$, and $CN^6Az$, as well as the 1,3-di-*tert*-butyl derivative of $CN^5Az$ ($CN^5Az^*$). These species represent the first examples of *organic* nonbenzenoid isocyanides.[18]

## Experimental Section

**General Procedures, Starting Materials, and Equipment.** Unless specified otherwise, all operations were performed under an atmosphere of 99.5% argon purified by passage through columns of activated BASF catalyst and molecular sieves. All connections involving the gas purification system were made of glass, metal, or other materials impermeable to air. Standard Schlenk techniques were employed with a double-manifold vacuum line. Solvents, including deuterated solvents, were freed of impurities by standard procedures and stored under argon.

Infrared spectra were recorded on a Thermo Nicolet Avatar 360 FTIR spectrometer with samples sealed in 0.1 mm gastight NaCl cells (solutions) or sandwiched between NaCl disks (neat films or Nujol mulls). Neat films for FTIR analysis were prepared by melting a solid sample placed directly between the NaCl disks. NMR samples were analyzed on Bruker DRX-400 and Bruker Avance 500 spectrometers. $^1H$ and $^{13}C$ chemical shifts are given with reference to residual $^1H$ and $^{13}C$ solvent resonances relative to $SiMe_4$. Such referencing eliminated bulk susceptibility effects for paramagnetic samples. Two-dimensional NMR techniques (DQF-COSY, $^1H-^{13}C$ HMQC, and $^1H-^{13}C$ HMBC)[19] were employed to obtain unambiguous assignments of $^1H$ and $^{13}C$ NMR resonances. The aromatic hydrogen resonances are labeled in reference to the corresponding carbon atoms (Figure 1). $^{14}N$ NMR chemical shifts

(8) Selected examples: (a) Wang, F.; Lai, Y.-H.; Han, M. Y. *Macromolecules* **2004**, *37*, 3222−3230. (b) Redl, F. X.; Köthe, O.; Röckl, K.; Bauer, W.; Daub, J. *Macromol. Chem. Phys.* **2000**, *201*, 2091−2100. (c) Feringa, B. L.; van Delden, R. A.; Koumura, N.; Geertsema, E. M. Chiroptical Molecular Switches. *Chem. Rev.* **2000**, *100*, 1789−1816.

(9) Selected examples: (a) Liu, R. S. H.; Asato, A. E. *J. Photochem. Photobiol. C* **2003**, *4*, 179−194. (b) Lambert, C.; Nöll, G.; Zabel, M.; Hampel, F.; Schmälzlin, E.; Bräuchle, C.; Meerholz, K. *Chem. Eur. J.* **2003**, *9*, 4232−4239. (c) Farrell, T., et al. *Dalton* **2001**, 29−36. (d) Lacroix, P. G.; Malfant, I.; Iftime, G.; Razus, A. C.; Nakatani, K.; Delaire, J. A. *Chem. Eur. J.* **2000**, *6*, 2599−2608. (e) Herrmann, R.; Pedersen, B.; Wagner, G.; Youn, J.-H. *J. Organomet. Chem.* **1998**, *571*, 261−266. (f) Cristian, L.; Sasaki, I.; Lacroix, P. G.; Donnadieu, B. *Chem. Mater.* **2004**, *16*, 3543−3551.

(10) (a) Ito, S.; Inabe, H.; Morita, N.; Ohta, K.; Kitamura, T.; Imafuku, K. *J. Am. Chem. Soc.* **2003**, *125*, 1669−1680. (b) Estdale, S. E.; Brettle, R.; Dunmur, D. A.; Marson, C. M. *J. Mater. Chem.* **1997**, *7*, 391−401.

(11) For example: (a) Möllerstedt, H.; Piqueras, M. C.; Crespo, R.; Ottosson, H. *J. Am. Chem. Soc.* **2004**, *126*, 13938−13939. (b) Stirling, A.; Iannuzzi, M.; Laio, A.; Parrinello, M. *Chemphyschem* **2004**, *5*, 1558−1568. (c) Alder, R. W.; East, S. P.; Harvey, J. N.; Oakley, M. T. *J. Am. Chem. Soc.* **2003**, *125*, 5375−5387.

(12) Selected examples: (a) Colby, D. A.; Ferrence, G. M.; Lash, T. D. *Angew. Chem., Int. Ed.* **2004**, *43*, 1346−1349. (b) Yeow, E. K. L.; Ziolek, M.; Karolczak, J.; Shevyakov, S. V.; Asato, A. E.; Maciejewski, A.; Steer, R. P. *J. Phys. Chem. A* **2004**, *108*, 10980−10988. (c) Wang, F.; Lai, Y. H.; Han, M. Y. *Org. Lett.* **2003**, *5*, 4791−4794.

(13) Selected examples: (a) Töfke, S.; Behrens, U. *Angew. Chem., Int. Ed. Engl.* **1987**, *26*, 147−148. (b) Churchill, M. R. *Prog. Inorg. Chem.* **1970**, *11*, 53−98.

(14) Fedushkin, I. L.; Bochkarev, M. N.; Mühle, S.; Schumann, H. *Russ. Chem. Bull., Int. Ed.* **2003**, *52*, 2005−2011.

(15) (a) De Sanctis, Y.; Arce, A. J.; Canavera, F.; Machado, R.; Deeming, A. J.; Gonzalez, T.; Galarza, E. *J. Organomet. Chem.* **2004**, *689*, 2025−2028. (b) Lash, T. D.; Colby, D. A.; Graham, S. R.; Ferrence, G. M.; Szczepura, L. F. *Inorg. Chem.* **2003**, *42*, 7326−7338.

(16) (a) Fabian, K. H. H.; Elwahy, A. H. M.; Hafner, K. *Tetrahedron Lett.* **2000**, *41*, 2855−2858. (b) Iyoda, M.; Kondo, T.; Okabe, T.; Matsuyama, H.; Sasaki, S.; Kuwatani, Y. *Chem. Lett.* **1997**, 35−36. (c) Ito, S.; Morita, N.; Asao, T. *J. Org. Chem.* **1996**, *61*, 5077−5082.

(17) Robinson, R. E.; Holovics, T. C.; Deplazes, S. F.; Lushington, G. H.; Powell, D. R.; Barybin, M. V. *J. Am. Chem. Soc.* **2003**, *125*, 4432−4433.

(18) Three *organometallic* isocyanides, namely isocyanoferrocene, 1,1′-diisocyanoferrocene, and isocyanocymantrene, are known: (a) Holovics, T. C.; Deplazes, S. F.; Toriyama, M.; Powell, D. R.; Lushington, G. H.; Barybin, M. V. *Organometallics* **2004**, *23*, 2927−2938. (b) Barybin, M. V.; Holovics, T. C.; Deplazes, S. F.; Lushington, G. H.; Powell, D. R.; Toriyama, M. *J. Am. Chem. Soc.* **2002**, *124*, 13668−13669. (c) van Leusen, D.; Hessen, B. *Organometallics* **2001**, *20*, 224−226. (d) Knox, G. R.; Pauson, P. L.; Willison, D.; Solcániová, E.; Toma, Š. *Organometallics* **1990**, *9*, 301−306. (e) El-Shihi, T.; Siglmüller, F.; Herrmann, R.; Carvalho, M. F. N. N.; Pombeiro, A. J. L. *J. Organomet. Chem.* **1987**, *335*, 239−247.

(19) Levitt, M. H. *Spin Dynamics: Basics of Nuclear Magnetic Resonance*; Wiley: New York, 2001.

are referenced to liquid $NH_3$ at 25 °C. UV−vis spectra were recorded in pentane at 24 °C using a Cary 100 spectrophotometer. Melting points are uncorrected and were determined for samples in sealed capillary tubes. Elemental analyses were carried out by Desert Analytics, Tucson, AZ. Mass spectral analyses were performed in the MS laboratory of the University of Kansas.

Azulene,[20] 2-aminoazulene,[21] 6-aminoazulene,[22] 1-nitroazulene,[23] 5-nitro-1,3-di-*tert*-butylazulene,[24] acetic-formic anhydride,[25] $V(CO)_6$,[26] bis($\eta^6$-naphthalene)chromium(0),[27] 1-cyanoazulene,[28] and $\beta$-isocyanonaphthalene[29] were prepared according to literature procedures or modified versions thereof. Other reagents were obtained from commercial sources.

**Magnetic Susceptibility Measurements.** Solid-state volume magnetic susceptibilities ($\chi_v$) were measured on a Johnson Matthey MSB-1 balance at ambient temperature and converted into the corresponding molar susceptibilities ($\chi_M$) in the usual manner.[30] Samples were packed into gastight tubes (0.400 cm o.d. × 0.324 cm i.d.) to a depth of ca. 3 cm in a drybox. The air correction of $0.029 \times 10^{-6}$ was applied to $\chi_v$ values of all samples packed under argon. Diamagnetic corrections applied to the $\chi_M$ values of the paramagnetic substances are reported as $\chi_{diam}$. These corrections were obtained by adding contributions from the $[BF_4]^-$ ($-39.0 \times 10^{-6}$ cm$^3$ mol$^{-1}$) or $[SbF_6]^-$ ($-80.0 \times 10^{-6}$ cm$^3$ mol$^{-1}$) ions to $\chi_M$ values of diamagnetic, low-spin $d^6$ complexes $Cr(CN^xAz)_6$ ($x = 1, 2, 4, 6$). The molar susceptibility of $Cr(CN^2Az)_6$ was *measured* to be $-211.2 \times 10^{-6}$ cm$^3$ mol$^{-1}$. Given the isomeric relationship of $Cr(CN^1Az)_6$, $Cr(CN^4Az)_6$, and $Cr(CN^6Az)_6$ with $Cr(CN^2Az)_6$, $\chi_M$ values of $Cr(CN^xAz)_6$ ($x = 1, 4, 6$) were assumed to be identical with that of $Cr(CN^2Az)_6$.

**1-Formamidoazulene ($^1$1).** Acetic-formic anhydride (3.0 mL), formic acid (3.0 mL), and tin powder (11.2 g, 95 mmol) were added to a blood red solution of 1-nitroazulene (2.73 g, 15.8 mmol) in 200 mL of toluene, and the mixture was warmed to 60 °C. After 1 h of stirring, additional portions of the anhydride (1.0 mL) and formic acid (1.0 mL) were introduced into the reaction flask. Heating was continued until the analysis by TLC (silica gel, $CHCl_3$) revealed complete consumption of 1-nitroazulene (ca. 2 h). The following workup was performed in air. The dark green mixture was cooled and poured into 400 mL of water. The organic phase was separated, and the aqueous layer was extracted with one portion of $CHCl_3$. The combined organic fractions were washed with saturated aqueous $K_2CO_3$ and dried over $Na_2SO_4$. Filtration followed by solvent removal afforded a dark green residue, which was subject to flash chromatography (silica gel, $CHCl_3$/$Et_2O$ = 3/1). Concentration of the green fraction afforded olive green **$^1$1** (2.067 g, 12.07 mmol) in a 77% yield. Mp: 106−108 °C. Anal. Calcd for $C_{11}H_9NO$: C, 77.17; H, 5.30; N, 8.18. Found: C, 76.88; H, 5.15; N, 8.07. $^{13}C\{^1H\}$ NMR (100.6 MHz, DMSO-$d^6$, 25 °C): $\delta$ 165.0, 159.5 (formyl *C*), 139.3, 138.5, 138.4, 137.6, 137.6, 133.1, 132.0, 131.2, 130.1, 129.6, 127.9, 123.4, 123.0, 122.8, 121.7, 116.2, 115.7 (azulenyl *C* atoms) ppm.

**2-Formamidoazulene ($^2$1).** A red solution of $H_2N^2Az$ (1.404 g, 9.760 mmol) in 15 mL of $CH_2Cl_2$ was treated with 5.0 mL of acetic-formic anhydride without protection from air. After it was stirred for 10 min at 20 °C, the reaction mixture was poured into 200 mL of water. The organic layer was separated, and the aqueous phase was extracted with $CH_2Cl_2$ (3 × 50 mL). The organic fractions were combined, washed with 100 mL of $H_2O$, and dried over $MgSO_4$. All solvent was then removed under reduced pressure. The residue was dried to give metallic lavender **$^2$1** (1.460 g, 8.528 mmol) in an 87% yield. Analytically pure **$^2$1** was furnished by passing a solution of **$^2$1** through a short column (silica gel, $CHCl_3/Et_2O$ = 4/1) with essentially no yield reduction. Mp: 194−196 °C. Anal. Calcd for $C_{11}H_9NO$: C, 77.17; H, 5.30; N, 8.18. Found: C, 77.40; H, 5.51; N, 8.39. $^{13}C\{^1H\}$ NMR (100.6 MHz, DMSO-$d^6$, 25 °C): $\delta$ 163.3, 159.8 (formyl *C*), 147.4, 145.4, 140.1, 139.5, 134.2, 133.8, 133.6, 132.8, 124.7, 124.1, 107.0, 103.7 (azulenyl *C* atoms) ppm.

**4-Formamidoazulene ($^4$1).** A solution of KO$^t$Bu (54.0 g, 481 mmol) in 300 mL of DMSO was rapidly transferred into a flask charged with azulene (5.120 g, 39.95 mmol), CuBr (0.500 g, 3.49 mmol), methoxyamine hydrochloride (10.1 g, 121 mmol), and DMSO (100 mL) at 20 °C. The mixture was stirred vigorously for a period of 4 h, during which time it acquired a dark red color, and then poured into 1.5 L of water and extracted with $CHCl_3$ (3 × 100 mL). The combined organic extracts were washed with water (3 × 100 mL) and dried over $Na_2SO_4$. All but 50 mL of the solvent was removed under vacuum, keeping the temperature below 35 °C. To this concentrated solution was added a large excess of acetic-formic anhydride (ca. 20 mL). The color of the reaction mixture immediately changed from red to purple. Following stirring for 10 min at 20 °C, the mixture was poured into a saturated aqueous solution of $Na_2CO_3$ (200 mL) and the layers were separated. The aqueous fraction was extracted once with 100 mL of $CHCl_3$. The organic fractions were combined and dried over $Na_2SO_4$. Filtration followed by solvent removal afforded a dark residue, which was then chromatographed on silica gel using neat $CHCl_3$. Two deep lavender bands were isolated. The first band provided pure, crystalline **$^4$1** (4.572 g, 26.71 mmol) in 67% yield upon solvent removal. Mp: 133−135 °C. Anal. Calcd for $C_{11}H_9NO$: C, 77.17; H, 5.30; N, 8.18. Found: C, 76.60; H, 5.15; N, 8.03. $^{13}C\{^1H\}$ NMR (100.6 MHz, $CDCl_3$, 25 °C): $\delta$ 163.6, 160.3 (formyl *C*), 141.1, 140.9, 138.2, 137.9, 137.2, 137.1, 136.7, 135.9, 134.9, 129.1, 122.5, 121.8, 121.2, 120.2, 118.3, 115.3, 113.8, 111.2 (azulenyl *C* atoms) ppm. The second band afforded a 17% yield of pure 6-formamidoazulene (1.154 g, 6.74 mmol) (vide infra).

**6-Formamidoazulene ($^6$1).** A red-maroon solution of 6-aminoazulene (0.858 g, 5.99 mmol) in 6 mL of $CH_2Cl_2$ was treated with 0.7 mL of acetic-formic anhydride without protection from air. After it was stirred for 10 min at 20 °C, the lavender reaction mixture was poured into 200 mL of water. The organic layer was separated, and the aqueous phase was extracted with $CH_2Cl_2$ (3 × 50 mL). The combined organic fractions were washed with water (100 mL) and dried over $MgSO_4$. Filtration followed by solvent removal afforded a dark lavender solid, which was dissolved in $CHCl_3$ and passed through a short silica gel column. The solvent was removed under vacuum to provide crystalline, dark lavender **$^6$1** in 94% yield (0.966 g, 5.64 mmol). Mp: 196−197 °C. Anal. Calcd for $C_{11}H_9NO$: C, 77.17; H, 5.30; N, 8.18. Found: C, 77.23; H, 5.16; N, 8.00. $^{13}C\{^1H\}$ NMR (100.6 MHz, DMSO-$d^6$, 25 °C): $\delta$ 163.6, 160.8 (formyl *C*), 146.9, 146.8, 137.1, 136.5, 134.4, 134.1, 119.2, 118.9, 118.8, 115.3, 114.5, 112.5 (azulenyl *C* atoms) ppm.

**5-Formamido-1,3-di-*tert*-butylazulene ($^5$1*).** Acetic-formic anhydride (2.0 mL), formic acid (0.8 mL), and tin powder (2.13 g, 17.9 mmol) were added to a dark green solution of 5-nitro-1,3-di-*tert*-butylazulene (0.500 g, 1.752 mmol) in 20 mL of toluene. The mixture was warmed to 60 °C. Heating was

(20) Hafner, K.; Meinhardt, K.-P. *Org. Synth.* **1984**, *62*, 134−139.
(21) Nozoe, T.; Matsumura, S.; Murase, Y.; Seto, S. *Chem. Ind. (London)* **1955**, 1257−1257.
(22) (a) Mąkosza, M.; Osiński, P. W.; Ostrowski, S. *Polish J. Chem.* **2001**, *75*, 275−281. (b) Mąkosza, M.; Podraza, R. *Eur. J. Org. Chem.* **2000**, 193−198.
(23) Anderson, A. G., Jr.; Scotoni, R., Jr.; Cowles, E. J.; Fritz, C. G. *J. Org. Chem.* **1957**, *22*, 1193−1196.
(24) Hafner, K.; Moritz, K. *Justus Liebigs Ann. Chem.* **1962**, *656*, 40−53.
(25) Krimen, L. I. *Org. Synth.* **1970**, *50*, 1−3.
(26) Liu, X.; Ellis, J. E. *Inorg. Synth.* **2004**, 96−103.
(27) Pomije, M. K.; Kurth, C. J.; Ellis, J. E.; Barybin, M. V. *Organometallics* **1997**, *16*, 3582−3587.
(28) Treibs, W.; Hiebsch, J.; Neupert, H.-J. *Chem. Ber.* **1959**, *92*, 606−615.
(29) Ugi, I.; Fetzer, U.; Eholzer, U.; Knupfer, H.; Offermann, K. *Angew. Chem., Int. Ed. Engl.* **1965**, *4*, 472−484.
(30) (a) Earnshaw, A. *Introduction to Magnetochemistry*; Academic Press: New York, 1968. (b) Kahn, O. *Molecular Magnetism*; VCH: New York, 1993.

continued until the analysis by TLC (silica gel, $CHCl_3$) revealed complete consumption of the starting material (ca. 2 h). The following workup was performed in air. The mixture was cooled and poured into 100 mL of water. The organic phase was separated, and the aqueous layer was extracted with three 20 mL portions of $CH_2Cl_2$. The combined organic fractions were washed with 20 mL of water and dried over anhydrous $Na_2SO_4$. Filtration followed by solvent removal afforded a dark aqua residue, which was subject to flash chromatography (silica gel, $CHCl_3/Et_2O$ = 4/1). Solvent removal from the aqua fraction afforded **$^5$1*** (0.361 g, 1.274 mmol) in 73% yield. Mp: 210−211 °C. HRMS (ES, positive *m/z*): calcd for $C_{19}H_{26}NO$ (M + 1), 284.2014; found, 284.2018(4). $^{13}C\{^1H\}$ NMR (100.6 MHz, $CDCl_3$, 25 °C): $\delta$ 164.4, 159.9 (formyl *C*), 138.2, 138.0, 137.6, 135.9, 133.9, 130.6, 130.1, 127.2, 118.9 (azulenyl *C* atoms), 33.7, 33.6, 32.6, 32.5 ($CH_3$) ppm.

**1-Isocyanoazulene ($^1$2).** Phosphorus oxychloride (1.14 mL, 12.2 mmol) was added over a 3 min period to a stirred solution of **$^1$1** (2.067 g, 12.07 mmol) and $^i$Pr$_2$NEt (3.0 mL, 18.1 mmol) in 25 mL of $CH_2Cl_2$ at 20 °C. After it was stirred for 10 min, the reaction mixture was quenched with 200 mL of 10% aqueous $K_2CO_3$. The following workup was performed in air. The organic layer was separated, and the aqueous layer was extracted with 50 mL of $CH_2Cl_2$. The combined organic fractions were washed with water (2 × 25 mL), dried over $Na_2SO_4$, filtered, and evaporated to dryness. The crude product was chromatographed on a short column (silica gel, $CHCl_3/Et_2O$ = 4/1) to elute a single, dark blue band. The solvent was removed, and the product was dried in vacuo to give royal blue **$^1$2** (1.636 g, 10.68 mmol) in 88% yield. Mp: 41−43 °C. Anal. Calcd for $C_{11}H_7N$: C, 86.25; H, 4.61; N, 9.14. Found: C, 86.13; H, 4.49; N, 9.16: IR (neat): $\nu_{CN}$ 2108 vs cm$^{-1}$. $^1$H NMR (400 MHz, $CDCl_3$, 25 °C): $\delta$ 7.23 (d, 1H, $H^3$, $^3J_{HH}$ = 4.2 Hz), 7.35 (dd, 1H, $H^5$, $^3J_{HH}$ = 9.9, 9.5 Hz), 7.38 (dd, 1H, $H^7$, $^3J_{HH}$ = 9.9, 9.5 Hz), 7.78 (t, 1H, $H^6$, $^3J_{HH}$ = 9.9 Hz), 7.83 (d, 1H, $H^2$, $^3J_{HH}$ = 4.2 Hz), 8.37 (d, 1H, $H^4$, $^3J_{HH}$ = 9.5 Hz), 8.50 (d, 1H, $H^8$, $^3J_{HH}$ = 9.5 Hz) ppm. $^{13}C\{^1H\}$ NMR (100.6 MHz, $CDCl_3$, 25 °C): $\delta$ 112.2 (t, $C^1$, $^1J_{CN}$ = 11.0 Hz) 115.6 ($C^3$), 124.9 ($C^7$), 125.8 ($C^5$), 132.9 ($C^2$), 134.1 ($C^9$), 134.4 ($C^8$), 138.6 ($C^{10}$), 139.3 ($C^4$), 139.9 ($C^6$), 166.6 (*C*NR) ppm. $^{14}$N NMR (36.2 MHz, $CDCl_3$, 25 °C): $\delta$ 169.9 ppm. UV−vis (pentane, $\lambda$ (log $\epsilon$)): 236 (4.36), 281 (4.72), 287 (4.67), 293 (4.72), 338 (3.70) sh, 346 (4.03), 354 (3.91) sh, 363 (4.10), 546 (2.07), 567 (2.21), 589 (2.33), 614 (2.26), 641 (2.27), 678 (1.28), 711 (1.43) nm.

**2-Isocyanoazulene ($^2$2)**. Dark blue **$^2$2** (0.840, 5.484 mmol) was prepared from **$^2$1** (1.020 g, 5.958 mmol), $^i$Pr$_2$NEt (3.0 mL, 18.1 mmol), and $POCl_3$ (0.546 mL, 5.8 mmol) in 92% yield by following the procedure described above for **$^1$2**. Mp: 70−73 °C. Anal. Calcd for $C_{11}H_7N$: C, 86.25; H, 4.61; N, 9.14. Found: C, 86.10; H, 4.37; N, 9.20. IR (neat): $\nu_{CN}$ 2118 vs cm$^{-1}$. $^1$H NMR (400 MHz, $CDCl_3$, 25 °C): $\delta$ 7.28 (s, 2H, $H^{1,3}$), 7.31 (t, 2H, $H^{5,7}$, $^3J_{HH}$ = 9.8 Hz), 7.70 (t, 1H, $H^6$, $^3J_{HH}$ = 9.8 Hz), 8.34 (d, 2H, $H^{4,8}$, $^3J_{HH}$ = 9.8 Hz) ppm. $^{13}C\{^1H\}$ NMR (100.6 MHz, $CDCl_3$, 25 °C): $\delta$ 114.0 ($C^{1,3}$), 125.4 ($C^{5,7}$), 130.4 (t, $C^2$, $^1J_{CN}$ = 11.2 Hz), 138.9 ($C^{9,10}$), 139.0 ($C^{4,8}$), 139.4 ($C^6$), 168.6 (t, *C*NR, $^1J_{CN}$ = 5.9 Hz) ppm. $^{14}$N NMR (36.2 MHz, $CDCl_3$, 25 °C): $\delta$ 175.3 ppm. UV−vis (pentane, $\lambda$ (log $\epsilon$)): 235 (4.52), 278 (4.89), 285 (4.89), 328 (4.20), 342 (4.21), 355 (4.18), 565 (2.44), 595 (2.39), 605 (2.43), 625 (1.99), 644 (1.64), 666 (1.86) nm.

**4-Isocyanoazulene ($^4$2).** Dark aqua **$^4$2** (0.876, 5.719 mmol) was prepared from **$^4$1** (1.040 g, 6.075 mmol), $^i$Pr$_2$NEt (3.0 mL, 18.1 mmol), and $POCl_3$ (0.70 mL, 7.5 mmol) in 94% yield by following the procedure described above for **$^1$2**. Mp: 39−40 °C. Anal. Calcd for $C_{11}H_7N$: C, 86.25; H, 4.61; N, 9.14. Found: C, 86.14; H, 4.38; N, 9.16. IR (neat): $\nu_{CN}$ 2117 vs cm$^{-1}$. $^1$H NMR (400 MHz, $CDCl_3$, 25 °C): $\delta$ 7.24 (d, 1H, $H^5$, $^3J_{HH}$ = 10.3 Hz), 7.28 (t, 1H, $H^7$, $^3J_{HH}$ ≈ 10 Hz), 7.50 (d, 1H, $H^1$, $^3J_{HH}$ = 3.7 Hz), 7.57 (t, 1H, $H^6$, $^3J_{HH}$ ≈ 10 Hz), 7.70 (d, 1H, $H^3$, $^3J_{HH}$ = 3.7 Hz), 8.02 (t, 1H, $H^2$, $^3J_{HH}$ = 3.7 Hz), 8.39 (d, 1H, $H^8$, $^3J_{HH}$ = 9.7 Hz) ppm. $^{13}C\{^1H\}$ NMR (100.6 MHz, $CDCl_3$, 25 °C): $\delta$ 117.5 ($C^1$), 121.1 ($C^3$), 121.4 ($C^5$), 124.2 ($C^7$), 129.9 (t, $C$,$^4$ $^1J_{CN}$ = 11.1 Hz), 132.8 ($C^{10}$), 135.4 ($C^6$), 137.2 ($C^8$), 138.9 ($C^2$), 141.0 ($C^9$), 167.6 (*C*NR) ppm. $^{14}$N NMR (36.2 MHz, $CDCl_3$, 25 °C): $\delta$ 181.8 ppm. UV−vis (pentane, $\lambda$ (log $\epsilon$)): 249 (4.71), 281 (4.84), 284 (4.82), 309 (3.33), 340 (3.37), 352 (3.51), 370 (3.06), 557 (2.18), 579 (2.31), 603 (2.59), 631 (2.53), 662 (2.58), 693 (2.31), 735 (2.32) nm.

**6-Isocyanoazulene ($^6$2).** Teal blue **$^6$2** (0.225 g, 1.47 mmol) was prepared from **$^6$1** (0.284 g, 1.66 mmol), $^i$Pr$_2$NEt (1.0 mL, 6.0 mmol), and $POCl_3$ (0.16 mL, 1.7 mmol) in 89% yield by following the procedure described above for **$^1$2**. Mp: 51−52 °C. Anal. Calcd for $C_{11}H_7N$: C, 86.25; H, 4.61; N, 9.14. Found: C, 86.51; H, 4.57; N, 9.01. IR (neat): $\nu_{CN}$ 2111 vs cm$^{-1}$. $^1$H NMR (400 MHz, $CDCl_3$, 25 °C): $\delta$ 7.21 (d, 2H, $H^{5,7}$, $^3J_{HH}$ = 10.2 Hz), 7.51 (d, 2H, $H^{1,3}$, $^3J_{HH}$ = 3.8 Hz), 8.01 (t, 1H, $H^2$, $^3J_{HH}$ = 3.8 Hz), 8.28 (d, 2H, $H^{4,8}$, $^3J_{HH}$ = 10.2 Hz) ppm. $^{13}C\{^1H\}$ NMR (100.6 MHz, $CDCl_3$, 25 °C): $\delta$ 121.0 ($C^{5,7}$), 121.3 ($C^{1,3}$), 133.0 ($C^6$), 135.2 ($C^{4,8}$), 139.8 ($C^2$), 140.1 ($C^{9,10}$), 164.7 (*C*NR) ppm. $^{14}$N NMR (36.2 MHz, $CDCl_3$, 25 °C): $\delta$ 186.6 ppm. UV−vis (pentane, $\lambda$ (log $\epsilon$)): 211 (4.14), 243 (4.05), 267 (4.35), 303 (3.61), 339 (3.51), 348 (3.71), 363 (3.43), 562 (2.67), 585 (2.70), 609 (2.74), 636 (2.67), 667 (2.68), 699 (2.43), 743 (2.41) nm.

**5-Isocyano-1,3-di-*tert*-butylazulene ($^5$2*).** Dark blue **$^5$2*** (0.636, 2.40 mmol) was prepared from **$^5$1*** (0.860 g, 3.03 mmol), $^i$Pr$_2$NH (3.0 mL, 21.3 mmol), and $POCl_3$ (0.30 mL, 3.2 mmol) in 79% yield by following the procedure described above for **$^1$2**. Mp: 154−157 °C. HRMS (ES, positive *m/z*): calcd for $C_{19}H_{24}N$ (M + 1), 266.1909, found, 266.1938(29). IR ($CHCl_3$): $\nu_{CN}$ 2114 vs cm$^{-1}$. $^1$H NMR (400 MHz, $CDCl_3$, 25 °C): $\delta$ 1.58 (s, 9H, $^tBu$), 1.60 (s, 9H, $^tBu$), 6.87 (dd, 1H, $H^7$, $^3J_{HH}$ = 10.0, 10.5 Hz), 7.51 (d, 1H, $H^6$, $^3J_{HH}$ = 10.0 Hz), 7.87 (s, 1H, $H^2$), 8.55 (d, 1H, $H^8$, $^3J_{HH}$ = 10.5 Hz), 8.58 (s, 1H, $H^4$) ppm. $^{13}C\{^1H\}$ NMR (100.6 MHz, $CDCl_3$, 25 °C): $\delta$ 32.3, 32.4 ($CH_3$), 33.6 ($CMe_3$), 33.7 ($CMe_3$), 117.7 (t, $C$,$^5$ $^1J_{CN}$ = 11.1 Hz), 118.6 ($C^7$), 132.5 ($C^{1or3}$), 132.9 ($C^6$), 134.4 ($C^4$), 135.5 ($C^8$), 136.2 ($C^{3or1}$), 137.7 ($C^2$), 141.2 ($C^{9or10}$), 141.4 ($C^{10or9}$), 160.8 (*C*NR) ppm. $^{14}$N NMR (36.2 MHz, $CDCl_3$, 25 °C): $\delta$ 184.7 ppm. UV−vis (pentane, $\lambda$ (log $\epsilon$)): 218 (4.17), 291 (4.61) br, 310 (3.85), 368 (3.93), 387 (4.11), 417 (2.75), 483 (2.74), 545 (2.76), 601 (2.82), 640 (2.79), 689 (2.63), 719 (2.62), 781 (2.21) nm.

**Cr(CN$^1$Az)$_6$ ($^1$3).** A royal blue solution of **$^1$2** (0.125 g, 0.816 mmol) in 20 mL of THF was added to a brown solution of Cr($\eta^6$-naphthalene)$_2$ (0.042 g, 0.136 mmol) in 20 mL of THF dropwise at −35 °C. The mixture was stirred for 15 h while being warmed to room temperature. Then heptane (50 mL) was added and the mixture was concentrated to ca. 60 mL to precipitate a deep purple solid. The solid was filtered off, washed with pentane (3 × 15 mL), and dried at $10^{-2}$ Torr to afford purple-black **$^1$3** (0.121 g, 0.125 mmol) in 92% yield. Mp: 195−199 °C dec. Anal. Calcd for $C_{66}H_{42}N_6Cr$: C, 81.63; H, 4.36; N, 8.65. Found: C, 81.27; H, 4.50; N, 8.24. IR (THF): $\nu_{CN}$ 1954 vs br cm$^{-1}$. $^1$H NMR (400 MHz, THF-$d_8$, 25 °C): $\delta$ 6.37 (t, 1H, $H^7$, $^3J_{HH}$ = 9.7 Hz), 6.93 (t, 1H, $H^5$, $^3J_{HH}$ = 9.7 Hz), 7.21 (d, 1H, $H^3$, $^3J_{HH}$ = 4.0 Hz), 7.27 (t, 1H, $H^6$, $^3J_{HH}$ = 9.7 Hz), 7.72 (d, 1H, $H^2$, $^3J_{HH}$ = 4.0 Hz), 8.11 (d, 1H, $H^4$, $^3J_{HH}$ = 9.7 Hz), 8.81 (d, 1H, $H^8$, $^3J_{HH}$ = 9.7 Hz) ppm. $^{13}C\{^1H\}$ NMR (100.6 MHz, THF-$d_8$, 25 °C): $\delta$ 115.0 ($C^3$), 118.2 ($C^{10}$), 121.8 ($C^7$), 123.6 ($C^5$), 130.0 ($C^2$), 133.5 ($C^8$), 134.6 ($C^9$), 137.0 ($C^4$), 137.5 ($C^1$), 138.8 ($C^6$), 200.6 (*C*NR) ppm.

**Cr(CN$^2$Az)$_6$ ($^2$3).** A deep blue solution of **$^2$2** (0.500 g, 3.26 mmol) in 20 mL of THF was added to a brown solution of Cr($\eta^6$-naphthalene)$_2$ (0.166 g, 0.538 mmol) in 20 mL of THF dropwise at room temperature. After the mixture was warmed to room temperature for 15 h, a dark blue solution/slurry formed. The mixture was filtered through a medium-porosity frit, and the blue-black solid was washed with THF (2 × 5 mL) and pentane (3 × 10 mL). After drying under vacuum, lustrous, blue-black **$^2$3** (0.492 g, 0.507 mmol) was isolated in 94% yield. The product decomposes above 300 °C without melting. Anal. Calcd for $C_{66}H_{42}N_6Cr$: C, 81.63; H, 4.36; N, 8.65. Found: C, 81.43; H, 4.43; N, 8.31. IR (Nujol mull): $\nu_{CN}$ 1954 vs br cm$^{-1}$.

**Cr(CN⁴Az)₆ (⁴3).** Purple-black **⁴3** (0.475 g, 0.489 mmol) was prepared from **⁴2** (0.500 g, 3.26 mmol) and Cr($\eta^6$-naphthalene)$_2$ (0.166 g, 0.538 mmol) in 91% yield by following the procedure described above for **¹3**. Mp: 139−142 °C dec. Anal. Calcd for $C_{66}H_{42}N_6Cr$: C, 81.63; H, 4.36; N, 8.65. Found: C, 81.33; H, 4.69; N, 8.56. IR (THF): $\nu_{CN}$ 1970 m sh, 1951 vs, 1938 m sh cm$^{-1}$. $^1$H NMR (500 MHz, THF-$d_8$, 25 °C): $\delta$ 7.06 (t, 1H, $H^7$, $^3J_{HH}$ = 9.7 Hz), 7.25 (d, 1H, $H^3$, $^3J_{HH}$ = 3.3 Hz), 7.29 (d, 1H, $H^5$, $^3J_{HH}$ = 9.7 Hz), 7.43 (dd, 1H, $H^2$, $^3J_{HH}$ = 3.3, 3.6 Hz), 7.46 (t, 1H, $H^6$, $^3J_{HH}$ = 9.7 Hz), 8.17 (d, 1H, $H^1$, $^3J_{HH}$ = 3.6 Hz), 8.27 (d, 1H, $H^8$, $^3J_{HH}$ = 9.7 Hz) ppm. $^{13}$C{$^1$H} NMR (125.8 MHz, THF-$d_8$, 25 °C): $\delta$ 118.2 ($C^1$) 120.7 ($C^3$), 121.8 ($C^5$), 122.7 ($C^7$), 134.5 ($C^{10}$), 134.7 ($C^4$), 136.0 ($C^2$), 136.5 ($C^6$), 137.6 ($C^8$), 140.5 ($C^9$), 198.3 (*C*NR) ppm. $^{14}$N NMR (36.2 MHz, THF-$d_8$, 25 °C): $\delta$ 198.8 ppm.

**Cr(CN⁶Az)₆ (⁶3).** Indigo-black **⁶3** (0.295 g, 0.304 mmol) was prepared in 76% yield by adding **⁶2** (0.401 g, 2.62 mmol) dissolved in 20 mL of THF to a solution of Cr($\eta^6$-naphthalene)$_2$ (0.123 g, 0.399 mmol) in 30 mL of THF via cannula at −78 °C. The workup was identical with that described above for the isolation of **²3**. Mp: 262 °C dec. Anal. Calcd for $C_{66}H_{42}N_6Cr$: C, 81.63; H, 4.36; N, 8.65. Found: C, 81.55; H, 4.19; N, 8.93. IR (Nujol mull): $\nu_{CN}$ 1950 vs br cm$^{-1}$.

**[Cr(CN¹Az)₆]⁺[BF₄]⁻ (¹3⁺[BF₄]⁻).** A deep purple solution of **¹3** (0.600 g, 0.618 mmol) in 30 mL of $CH_2Cl_2$ was added to a slurry of $AgBF_4$ (0.122 g, 0.627 mmol) in 50 mL of $CH_2Cl_2$ via cannula at −78 °C. The mixture turned brown within minutes and was stirred for 1 h while being warmed to room temperature. Then, the contents of the reaction flask were filtered through a 3 cm plug of Celite to remove Ag metal. The filter cake was washed with an additional 75 mL of $CH_2Cl_2$. The filtrate was concentrated to ca. 5 mL under vacuum. Pentane (40 mL) was then added to precipitate brown microcrystals. These were filtered off, washed with pentane (3 × 15 mL), and dried at $10^{-2}$ Torr to afford **¹3**$^+$[$BF_4$]$^-$ (0.481 g, 0.455 mmol) in 74% yield. Mp: 218−223 °C dec. Anal. Calcd for $C_{66}H_{42}N_6BCrF_4$: C, 74.93; H, 4.00; N, 7.94. Found: C, 74.61; H, 4.09; N, 7.63. IR ($CH_2Cl_2$): $\nu_{CN}$ 2034 vs; $\nu_{BF}$ 1061 m br cm$^{-1}$. $^1$H NMR (400 MHz, $CD_2Cl_2$, 25 °C): $\delta$ −6.38 (s br, 1H, $H^7$), −4.81 (t, 1H, $H^5$, $^3J_{HH}$ = 9.5 Hz), −2.69 (s br, 1H, $H^2$), 8.20 (s br, 1H, $H^3$), 11.35 (d, 1H, $H^4$, $^3J_{HH}$ = 9.5 Hz), 12.21 (t, 1H, $H^6$, $^3J_{HH}$ = 9.5 Hz), 13.58 (s br, 1H, $H^8$) ppm. $^{13}$C{$^1$H} NMR (100.6 MHz, $CD_2Cl_2$, 25 °C): $\delta$ 56.4 ($C^8$), 79.9 ($C^6$), 82.7 ($C^3$), 86.9 ($C^4$), 162.7 ($C^{10}$), 195.0 ($C^5$), 197.8 ($C^2$), 204.4 ($C^7$), 215.0 ($C^9$) ppm. $^{14}$N NMR (36.2 MHz, $CD_2Cl_2$, 25 °C): $\delta$ 813.5 ppm. $\mu_{eff}$(24.0 °C) = 2.07 $\mu_B$ ($\chi_{diam}$ = −250.2 × $10^{-6}$ cm$^3$ mol$^{-1}$).

**[Cr(CN¹Az)₆]⁺[V(CO)₆]⁻ (¹3⁺[V(CO)₆]⁻).** A freshly prepared yellow solution of $V(CO)_6$ (0.034 g, 0.155 mmol) in 20 mL of $CH_2Cl_2$ was added to a deep purple solution of **¹3** (0.150 g, 0.154 mmol) in 50 mL of $CH_2Cl_2$ via cannula at 20 °C. The reaction mixture acquired a brown color within minutes. After it was stirred for 2 h, the mixture was filtered through a 3 cm plug of Celite. The filter cake was washed with an additional 60 mL of $CH_2Cl_2$. All but ca. 5 mL of the solvent was removed under vacuum, and 50 mL of heptane was added to the concentrated filtrate to precipitate brown microcrystals. These were washed with pentane (3 × 15 mL), recrystallized from $CH_2Cl_2$/pentane, and dried at $10^{-2}$ Torr to afford **¹3**$^+$[$V(CO)_6$]$^-$ (0.104 g, 0.087 mmol) in 56% yield. IR ($CH_2Cl_2$): $\nu_{CN}$ 2033 vs; $\nu_{CO}$ 1853 vs cm$^{-1}$. The $^1$H and $^{13}$C NMR ($CD_2Cl_2$, 25 °C) spectra for the cation in **¹3**$^+$[$V(CO)_6$]$^-$ were identical to those reported above for **¹3**$^+$[$BF_4$]$^-$.

**[Cr(CN²Az)₆]⁺[BF₄]⁻ (²3⁺[BF₄]⁻).** Dichloromethane (30 mL) was added to a solid mixture of **²3** (0.213 g, 0.219 mmol) and finely ground $AgBF_4$ (0.048 g, 0.247 mmol) at 20 °C. The slurry turned deep purple within minutes. The mixture was stirred for 15 h and then filtered trough a 3 cm plug of Celite. An additional 50 mL of $CH_2Cl_2$ was employed to wash the filter cake. All but ca. 10 mL of the solvent was removed, and 40 mL of pentane was added to precipitate deep purple microcrystals. These were washed with pentane (2 × 15 mL) and dried under vacuum to afford **²3**$^+$[$BF_4$]$^-$ (0.176 g, 0.166 mmol) in 76% yield. The product decomposes above 300 °C without melting. Anal. Calcd for $C_{66}H_{42}N_6BCrF_4$: C, 74.93; H, 4.00; N, 7.94. Found: C, 74.60; H, 3.92; N, 7.66. IR ($CH_2Cl_2$): $\nu_{CN}$ 2062 vs sh, 2047 vs; $\nu_{BF}$ 1031 m br cm$^{-1}$. $^1$H NMR (400 MHz, $CD_2Cl_2$, 25 °C): $\delta$ −0.24 (s, 2H, $H^{1,3}$), 4.16 (t, 1H, $H^6$, $^3J_{HH}$ = 9.7 Hz), 5.47 (d, 2H, $H^{4,8}$, $^3J_{HH}$ = 9.7 Hz), 9.47 (d, 2H, $H^{5,7}$, $^3J_{HH}$ = 9.7 Hz) ppm. $^{13}$C{$^1$H} NMR (100.6 MHz, $CD_2Cl_2$, 25 °C): $\delta$ −44.6 ($C^2$), 107.8 ($C^{5,7}$), 116.2 ($C^{9,10}$), 162.3 ($C^6$), 166.5 ($C^{4,8}$), 226.1 ($C^{1,3}$) ppm. $^{14}$N NMR (36.2 MHz, $CD_2Cl_2$, 25 °C): $\delta$ 859.6 ppm. $\mu_{eff}$(25.0 °C) = 1.73 $\mu_B$ ($\chi_{diam}$ = −250.2 × $10^{-6}$ cm$^3$ mol$^{-1}$).

**[Cr(CN⁴Az)₆]⁺[SbF₆]⁻ (⁴3⁺[SbF₆]⁻).** Brown-black microcrystals of **⁴3**$^+$[$SbF_6$]$^-$ (0.215 g, 0.184 mmol) were obtained from **⁴3** (0.200 g, 0.206 mmol) and $AgSbF_6$ (0.074 g, 0.215 mmol) in 89% yield by following the procedure described above for **²3**$^+$[$BF_4$]$^-$. Mp: 188−190 °C dec. Anal. Calcd for $C_{66}H_{42}N_6CrF_6Sb$: C, 65.69; H, 3.51; N, 6.96. Found: C, 65.24; H, 4.00; N, 6.70. IR ($CH_2Cl_2$): $\nu_{CN}$ 2050 vs cm$^{-1}$. $^1$H NMR (500 MHz, $CD_2Cl_2$, 24 °C): $\delta$ 0.55 (d, 1H, $H^5$, $^3J_{HH}$ = 9.5 Hz), 3.53 (t, 1H, $H^7$, $^3J_{HH}$ = 9.5 Hz), 4.58 (s br, 1H, $H^2$), 8.69 (s br, 1H, $H^1$), 9.98 (s br, 1H, $H^3$), 10.34 (d, 1H, $H^8$, $^3J_{HH}$ = 9.5 Hz), 12.11 (t, 1H, $H^6$, $^3J_{HH}$ = 9.5 Hz) ppm. $^{13}$C{$^1$H} NMR (125.8 MHz, $CD_2Cl_2$, 24 °C): $\delta$ 97.0 ($C^1$), 111.7 ($C^3$), 113.8 ($C^6$), 120.1 ($C^8$), 150.0 ($C^7$), 155.9 ($C^2$), 158.1 ($C^9$), 195.0 ($C^5$) ppm. $^{14}$N NMR (36.2 MHz, $CD_2Cl_2$, 25 °C): $\delta$ 831.5 ppm. $\mu_{eff}$(24.0 °C) = 1.80 $\mu_B$ ($\chi_{diam}$ = −291.2 × $10^{-6}$ cm$^3$ mol$^{-1}$).

**[Cr(CN⁶Az)₆]⁺[BF₄]⁻ (⁶3⁺[BF₄]⁻).** Deep purple leaflets of **⁶3**$^+$[$BF_4$]$^-$ (0.175 g, 0.165 mmol) were obtained from **⁶3** (0.500 g, 3.26 mmol) and finely ground $AgBF_4$ (0.053 g, 0.270 mmol) in 64% yield using the procedure described for **²3**$^+$[$BF_4$]$^-$. The product decomposes above 300 °C without melting. Anal. Calcd for $C_{66}H_{42}N_6BCrF_4$: C, 74.93; H, 4.00; N, 7.94. Found: C, 74.60; H, 3.84; N, 7.98. IR ($CH_2Cl_2$): $\nu_{CN}$ 2053 vs; $\nu_{BF}$ 1031 m br cm$^{-1}$. $^1$H NMR (400 MHz, $CD_2Cl_2$, 25 °C): $\delta$ 0.63 (d, 2H, $H^{5,7}$, $^3J_{HH}$ = 9.3 Hz), 3.99 (t, 1H, $H^2$, $^3J_{HH}$ = 3.5 Hz), 8.75 (d, 2H, $H^{1,3}$, $^3J_{HH}$ = 3.5 Hz), 12.71 (d, 2H, $H^{4,8}$, $^3J_{HH}$ = 9.3 Hz) ppm. $^{13}$C{$^1$H} NMR (100.6 MHz, $CD_2Cl_2$, 25 °C): $\delta$ −27.0 ($C^6$), 104.6 ($C^{1,3}$), 117.4 ($C^{4,8}$), 155.8 ($C^{9,10}$), 164.0 ($C^2$), 251.6 ($C^{5,7}$) ppm. $^{14}$N NMR (36.2 MHz, $CD_2Cl_2$, 25 °C): $\delta$ 832 ppm. $\mu_{eff}$(24.5 °C) = 1.71 $\mu_B$ ($\chi_{diam}$ = −250.2 × $10^{-6}$ cm$^3$ mol$^{-1}$).

**X-ray Work.** X-ray-quality crystals of **¹3**$^+$[$V(CO)_6$]$^-$, **²3**$^+$[$BF_4$]$^-$·0.915$CH_2Cl_2$·0.301$C_5H_{12}$, **⁴3**$^+$[$SbF_6$]$^-$, and **⁶3**$^+$[$BF_4$]$^-$ were grown at 4 °C by carefully layering pentane over $CH_2Cl_2$ solutions of the corresponding complexes. Intensity data were collected using a Bruker APEX CCD area detector mounted on a Bruker D8 goniometer. Graphite-monochromated Mo Kα radiation ($\lambda$ = 0.710 73 Å) was employed. All structures were solved by direct methods and refined by full-matrix least-squares methods on $F^2$ using the SHELXTL V5.0 suite of programs. The details of the X-ray diffraction experiments are summarized in Table 1. Full description of the crystallographic work is available in the Supporting Information.

**Electrochemical Measurements.** Cyclic voltammetric experiments on 2 × $10^{-3}$ M solutions of analytes in $CH_2Cl_2$ were conducted in a drybox at 22 ± 2 °C using an EPSILON (Bioanalytical Systems Inc., West Lafayette, IN) electrochemical workstation. The supporting electrolyte was 0.1 M [$^n$$Bu_4N$]-[$PF_6$] in $CH_2Cl_2$. A three-component system consisting of a platinum working electrode, a platinum-wire auxiliary electrode, and a glass-encased nonaqueous Ag/AgCl reference electrode was used. The electrochemical setup and procedure were identical with those recently reported elsewhere[18a] and are also described in the Supporting Information. The reported potentials were determined at a scan rate of 100 mV/s.

**DFT Calculations.** Density functional theory (DFT) electronic structure calculations on **$^x$2** ($x$ = 1, 2, 4−6) were carried out with the Gaussian 98 program[31] using the B3LYP func-

(31) Frisch, M. J.; et al. Gaussian 98 (Revision A.10). Gaussian, Inc., Pittsburgh, PA, 1998.

**Table 1. X-ray Crystallographic Information for $^{1}$**3**$^{+}$[V(CO)$_6$]$^{-}$, $^{2}$**3**$^{+}$[BF$_4$]$^{-}$·0.915CH$_2$Cl$_2$·0.301C$_5$H$_{12}$, $^{4}$**3**$^{+}$[SbF$_6$]$^{-}$, and $^{6}$**3**$^{+}$[BF$_4$]$^{-}$**

| | $^{1}$**3**$^{+}$[V(CO)$_6$]$^{-}$ | $^{2}$**3**$^{+}$[BF$_4$]$^{-}$·0.915CH$_2$Cl$_2$·0.301C$_5$H$_{12}$ | $^{4}$**3**$^{+}$[SbF$_6$]$^{-}$ | $^{6}$**3**$^{+}$[BF$_4$]$^{-}$ |
|---|---|---|---|---|
| empirical formula | $C_{72}H_{42}CrN_6O_6V$ | $C_{68.42}H_{47.44}BCl_{1.83}CrF_4N_6$ | $C_{66}H_{42}CrF_6N_6Sb$ | $C_{66}H_{42}BCrF_4N_6$ |
| formula wt | 1190.06 | 1157.29 | 1576.80 | 1057.87 |
| space group | $R\bar{3}$ | $P\bar{1}$ | $P\bar{1}$ | $C2/c$ |
| $a$ (Å) | 14.7896(9) | 12.6091(9) | 10.1697(11) | 19.934(7) |
| $b$ (Å) | 14.7896(9) | 15.2331(11) | 11.5363(12) | 13.572(5) |
| $c$ (Å) | 22.454(3) | 16.3811(11) | 13.1899(14) | 21.073(7) |
| α (deg) | 90 | 78.316(2) | 70.228(2) | 90 |
| $\beta$ (deg) | 90 | 67.579(2) | 75.234(2) | 106.973(6) |
| $\gamma$ (deg) | 120 | 80.723(2) | 68.273(2) | 90 |
| V (Å$^3$) | 4253.4(7) | 2836.0(3) | 1337.8(2) | 5453(3) |
| $Z$, $Z'$ | 3, 0.166 667 | 2, 1 | 1, 0.5 | 4, 0.5 |
| $\rho_{calcd}$ (Mg m$^{-3}$) | 1.394 | 1.355 | 1.498 | 1.289 |
| $\mu$ (mm$^{-1}$) | 0.419 | 0.350 | 0.778 | 0.271 |
| temp (K) | 100(2) | 100(2) | 100(2) | 100(2) |
| $R_{int}$[a] | 0.0228 | 0.0196 | 0.0234 | 0.1797 |
| R1;[b] wR2[c] | 0.0390; 0.1114 | 0.0546; 0.1576 | 0.0558; 0.1532 | 0.0641; 0.1733 |
| GOF on $F^2$ | 1.068 | 1.066 | 1.002 | 0.969 |

[a] $R_{int} = \Sigma|F_o^2 - \langle F_o^2\rangle|/\Sigma|F_o^2|$. [b] $R1 = \Sigma||F_o| - |F_c||/\Sigma|F_o|$. [c] $wR2 = [\Sigma(w(F_o^2 - F_c^2)^2)/\Sigma(w(F_o^2)^2)]^{1/2}$.

tional[32] and 6-31G(d,p) basis set. The geometry of each molecule was optimized, and identification of the minimum was confirmed by a frequency calculation. Vertical excitation energies were obtained using time-dependent DFT[33] with the Q-Chem program.[34] Calculations on the complexes $^{1}$**3**$^{+}$ and $^{6}$**3**$^{+}$ were carried out at the B3LYP/STO-3G level.[35] Further details of the calculations are available in the Supporting Information.

## Results and Discussion

**Isocyanoazulenes.** Organic isocyanides (:C≡NR), also referred to as isonitriles or carbylamines, are among the few isolable species possessing a lone electron pair on a carbon atom. The most general route to these highly reactive substances involves formylation of the corresponding primary amine, $H_2NR$, followed by dehydration of the resulting formamide, H(O)CNHR.[36] While aminoazulenes $H_2N^xAz$ ($x$ = 1, 2, 4, 6) have been known for decades,[3] their synthetic use has been hampered by notorious instability[37] of all $H_2N^xAz$ as well as poor yields associated with the preparation of $H_2N^4Az$ and $H_2N^6Az$.[38] Recently, Mąkosza et al. have described an elegant direct amination of azulene with 4-amino-1,2,4-triazole, which provided $H_2N^6Az$ in practical quantities and yield.[22] The same authors have also reported that treatment of azulene with methoxyamine in the presence of $^t$BuOK and CuCl afforded an inseparable mixture (25 mg) of $H_2N^4Az$ and $H_2N^6Az$, which formed in 20 and 15% yields, respectively.[22a] We modified the latter synthesis by employing CuBr as a catalyst and using excess amounts of $^t$BuOK and MeONH$_2$·HCl to increase the overall amination yield to at least 84%, while tripling the selectivity of amination in favor of $H_2N^4Az$ production.[39]

The syntheses of 1-, 2-, 4-, and 6-formamidoazulenes ($^{1}$**1**, $^{2}$**1**, $^{4}$**1**, and $^{6}$**1**) are summarized in eqs 1−4. Due to

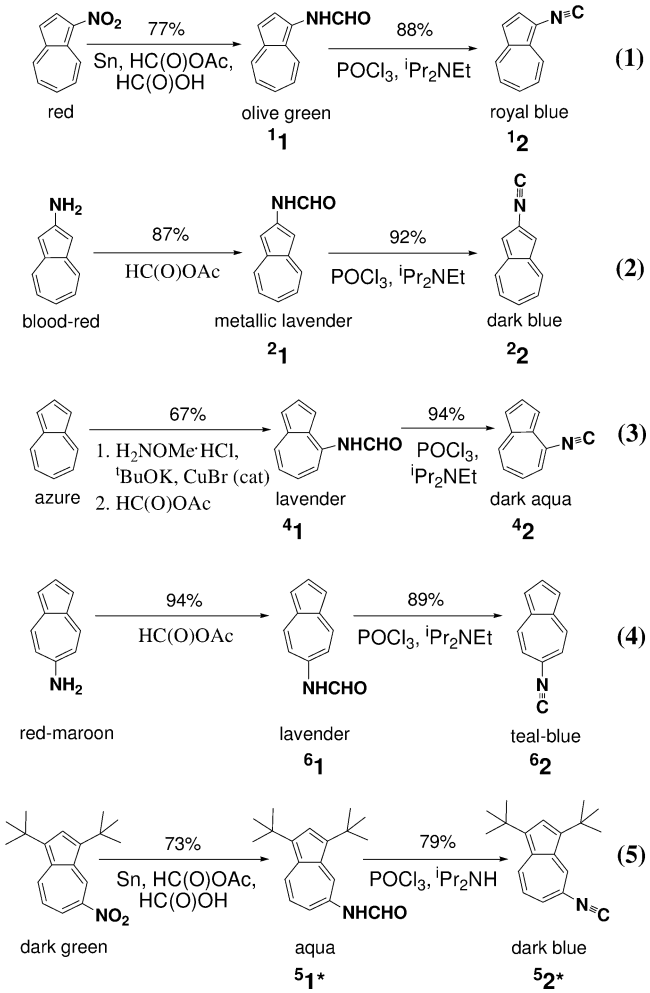


the exceedingly poor thermal stability of $H_2N^1Az$,[3a,9e] a direct route to H(O)CNH$^1$Az ($^{1}$**1**) from $O_2N^1Az$ that employs reductive formylation conditions was devised (eq 1). In the preparation of $^{4}$**1** (eq 3), a small amount

(32) (a) Miehlich, B.; Savin, A.; Stoll, H.; Preuss, H. *Chem. Phys. Lett.* **1989**, *157*, 200−206. (b) Lee, C.; Yang W.; Parr, R. G. *Phys. Rev. B* **1988**, *37*, 785−789.

(33) (a) Runge, E.; Gross, E. K. U. *Phys. Rev. Lett*. **1984**, *52*, 997−1000. (b) Hirata, S.; Head-Gordon, M. *Chem. Phys. Lett*. **1999**, *302*, 375−382.

(34) Kong, J.; et al. *J. Comput. Chem.* **2000**, *21*, 1532−1548.

(35) Stewart, R. F. *J. Chem. Phys.* **1970**, *52*, 431−438.

(36) Ugi, I. *Isonitrile Chemistry*; Academic Press: New York, 1971.

(37) In our experience, *pure crystalline* samples of $H_2N^2Az$ and $H_2N^6Az$ are storable at −30 °C for months without significant deterioration. Crude $H_2N^2Az$ and $H_2N^6Az$ are much more prone to decomposition, especially if acidic impurities are present.

(38) (a) Reid, D. H.; Stafford, W. H.; Ward, J. P. *J. Chem. Soc.* **1958**, 1100−1109. (b) Nozoe, T.; Takase, K.; Tada, M. *Bull. Chem. Soc. Jpn.* **1963**, *36*, 1006−1009.

(39) See preparation of $^{4}$**1** in the Experimental Section.

**Table 2. Comparison of $\nu_{CN}$ Values ($cm^{-1}$) for Isocyanoazulenes, Cyanoazulenes, Isocyanonaphthalenes, and Cyanonaphthalenes**

| | R | | | | | | |
|---|---|---|---|---|---|---|---|
| | $^{\beta}$Naph | $^{\alpha}$Naph | $^{2}$Az | $^{4}$Az | $^{5}$Az$^{*}$ | $^{6}$Az | $^{1}$Az |
| CNR | 2123[a,c] | 2119[a,d] | 2118[a,c] | 2117[a,c] | 2114[a,c] | 2111[a,c] | 2108[a,c] |
| NCR | 2228[b,e] | 2223[b,e] | 2223[b,f] | 2220[b,g] | | 2212[a,h] | 2207[a,c] |

[a] Neat film. [b] KBr. [c] This work. [d] Reference 44. [e] Reference 45. [f] Reference 46. [g] Reference 47. [h] Reference 48.

of $^{6}$**1** was also produced. Unlike $H_2N^4Az$ and $H_2N^6Az$, $^{4}$**1** and $^{6}$**1** were easily separable by chromatography.[39] In solution, the compounds $^{x}$**1** ($x$ = 1, 2, 4, 6) exist as mixtures of two conformational isomers, owing to the restricted rotation[40] around the H(O)C−NH$^x$Az bonds. The nearly quantitative dehydrations of $^{x}$**1** ($x$ = 1, 2, 4, 6) to afford the corresponding isocyanoazulenes $^{x}$**2** were effected by $POCl_3$ (eqs 1−4). The synthesis of the remaining fifth archetypal isocyanoazulene, CN$^5$Az, proved to be the most challenging and is currently in progress. This species cannot be accessed from azulene itself, because the azulenic carbon atoms 1 and 3 are far more susceptible to an electrophilic attack than those in positions 5 and 7. Nevertheless, we succeeded in isolating a bis-alkyl derivative of CN$^5$Az, $^{5}$**2**$^{*}$ (the asterisk refers to $^{t}$Bu substitution of the Az group at positions 1 and 3), via reductive formylation of 5-nitro-1,3-di-*tert*-butylazulene followed by dehydration of the resulting formamide $^{5}$**1**$^{*}$ (eq 5).

The isocyanoazulenes described herein are highly colored, crystalline substances with relatively mild odor ($^{2}$**2** and $^{6}$**2** are virtually odorless). They do not rearrange into cyanoazulenes upon moderate heating (ca. 70 °C). Of all five, only $^{6}$**2** appears to be slightly air-sensitive.[41] The above properties are in sharp contrast to those of many benzenoid isocyanides, which have a pungent odor, deteriorate rapidly upon exposure to air,[42] and isomerize into the corresponding cyanides at 40−50 °C.[43] For instance, α-isocyanonaphthalene (CN$^{\alpha}$Naph, a benzenoid isomer of $^{x}$**2**), is an air- and thermally sensitive, malodorous liquid, the dark brown color[44] of which is almost certainly associated with persistent contamination with oligomerized CN$^{\alpha}$Naph.

The isocyanides $^{1}$**2**, $^{2}$**2**, $^{4}$**2**, $^{5}$**2**$^{*}$, and $^{6}$**2** can be easily distinguished from the corresponding cyanide species on the basis of their characteristic features in IR ($\nu_{CN}$ 2108−2118 $cm^{-1}$), $^{13}$C NMR ($\delta$(*C*NAz) 165−169 ppm), and $^{14}$N NMR ($\delta$ 170−187 ppm) spectra. The C≡N stretching frequencies determined for the five isocyanoazulenes are somewhat lower than those recorded for α- and $\beta$-isocyanonaphthalenes under the same conditions (Table 2). This fact may be attributed to slightly more effective conjugation between the −NC group and the azulenyl rather than naphthyl fragment due to lower aromatic stabilization of the nonbenzenoid azulenic moiety.[49] The $\nu_{CN}$ energies observed for the isocyanoazulenes decrease in the order $^{2}$**2** ≥ $^{4}$**2** > $^{5}$**2*** > $^{6}$**2** > $^{1}$**2**. Compounds $^{1}$**2** and $^{6}$**2** exhibit the lowest $\nu_{CN}$ values documented for an aryl isocyanide, to the best of our knowledge. Interestingly, cyanoazulenes show the same trend in sensitivity of $\nu_{CN}$ to the position of the CN group attachment (Table 2).

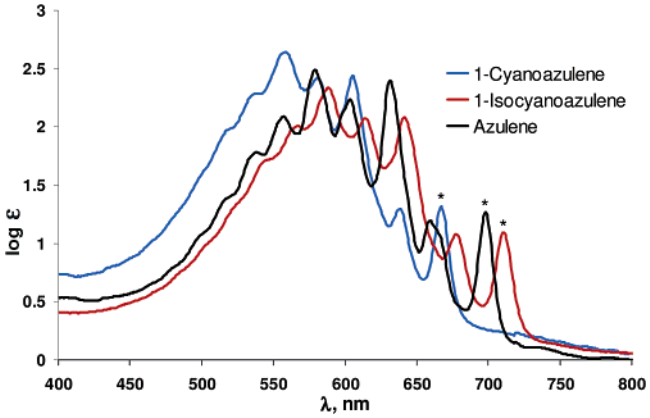


**Figure 3.** Long-wave absorption bands of 1-cyanoazulene, 1-isocyanoazulene, and azulene, all recorded in pentane at 24 °C. The 0 → 0 transitions are labeled with asterisks.

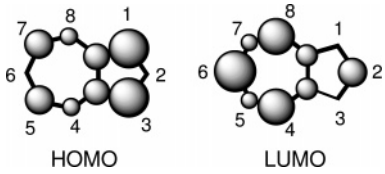


**Figure 4.** Schematic representation of azulene's HOMO and LUMO. The circles indicate squares of atomic orbital coefficients.[48]

The absorption spectra of $^{1}$**2**, $^{2}$**2**, $^{4}$**2**, $^{5}$**2**$^{*}$, and $^{6}$**2** in pentane exhibit a structural band in the visible region with $\lambda_{max}$ ranging from 565 to 609 nm. This transition is due to the HOMO → LUMO excitation, which for azulene itself occurs at $\lambda_{max}$ 579 nm ($^1$A → $^1$L$_b$) in the same solvent (Figure 3). Unlike alternant aromatics (e.g., naphthalene), nonalternant azulene can experience both widening and shrinking of the HOMO−LUMO gap upon substitution, depending on the substituent's nature and position of its attachment.[3a,50] Given uneven electron density distributions within azulene's HOMO and LUMO (Figure 4), it has been argued that incorporation of an unsaturated electron-withdrawing group (EWG) at carbon atoms 2, 4, or 6 should lead to a bathochromic (red) shift of azulene's $^1$A → $^1$L$_b$ band because of stabilization of the LUMO through both conjugation and inductive effects, while not significantly affecting the HOMO level.[3a,50] On the other hand, this EWG at an odd-numbered carbon atom of azulene will affect its HOMO, but not LUMO, in two mutually opposing ways: destabilization due to conjugation with the substituent and stabilization caused by the sub-

(40) Kessler, H. *Angew. Chem., Int. Ed. Engl.* **1970**, *9*, 219−235.
(41) While $^{6}$**2** can be handled on air for hours without noticeable degradation, we recommend placing it under an inert atmosphere at −20 °C for long-term storage.
(42) Malatesta, L. *Prog. Inorg. Chem.* **1959**, *1*, 283−379.
(43) Meier, M.; Mueller, B.; Ruechardt, C. *J. Org. Chem.* **1987**, *52*, 648−652.
(44) Lim, Y.-M.; Park, H.-S.; Song, S.-H.; Park, C.-J.; Ryu, H.; Jee, J.-G.; Yang, H.-S. *Bull. Korean Chem. Soc.* **1999**, *20*, 701−704.
(45) SDBS Database: www.aist.go.jp/RIODB/SDBS/menu-e.html.
(46) Nozoe, T.; Seto, S.; Matsumura, S. *Bull. Chem. Soc. Jpn.* **1962**, *35*, 1990−1998.
(47) Hünig, S.; Hafner, K.; Ort, B.; Müller, M. *Liebigs Ann. Chem.* **1986**, 1222−1240.
(48) McDonald, R. N.; Richmond, J. M.; Curtis, J. R.; Petty, H. E.; Hoskins, T. L. *J. Org. Chem.* **1976**, *41*, 1811−1821.
(49) Wang, P.; Zhu, P.; Ye, C.; Asato, A. E.; Liu, R. S. H. *J. Phys. Chem. A* **1999**, *103*, 7076−7082.
(50) Shevyakov, S. V.; Li, H.; Muthyala, R.; Asato, A. E.; Croney, J. C.; Jameson, D. M.; Liu, R. S. H. *J. Phys. Chem. A* **2003**, *107*, 3295−3299.

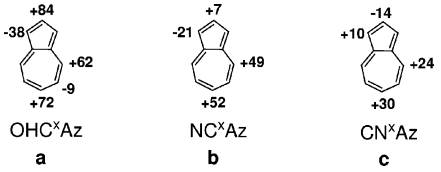


**Figure 5.** Shifts (in nm) of $\lambda_{max}$ of the $^1A \rightarrow {}^1L_b$ band upon substitution of azulene with (a) formyl, (b) cyano, and (c) isocyano groups at various positions.[51]

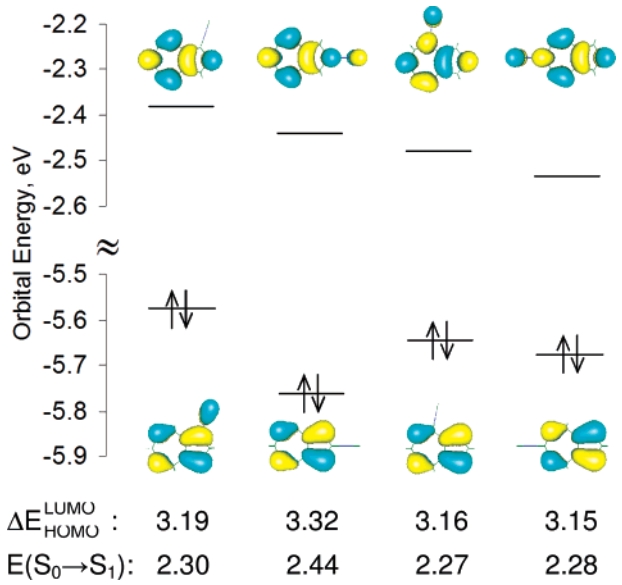


**Figure 6.** From left to right: HOMO's and LUMO's of **$^1$2**, **$^2$2**, **$^4$2**, and **$^6$2**. The corresponding HOMO−LUMO gaps (eV) and TD-DFT excitation energies ($S_0 \rightarrow S_1$, eV) are listed at the bottom of the diagram.[52]

stituent's positive inductive influence. The inductive effect prevails for strong EWG's, thereby resulting in a hypsochromic (blue) shift of the $^1A \rightarrow {}^1L_b$ band.[3a,50] This rationale has been confirmed experimentally by considering, for example, five isomeric formylazulenes (Figure 5a).[50] The same argument seems to hold for 1-, 2-, 4-, and 6-cyanoazulenes (Figure 5b). Notably, 5-cyanoazulene is not known.

Since −NC is perceived[18e,36] to be a rather potent EWG (e.g., see dipole moment data in Figure 2), we were surprised to discover that the above long-accepted rationale failed when applied to the isocyanoazulene family, particularly **$^1$2** and **$^2$2** (Figure 5c). While the red shift of the low-energy band observed for **$^1$2** can, in principle, be explained by invoking dominance of the conjugation effect, the shift of the same band for **$^2$2** is blue, which contradicts the expectations regardless of the relative magnitudes of inductive and resonance effects. To address this discrepancy, we turned to the DFT analysis of ***x*2** summarized in Figure 6. The relative HOMO−LUMO gaps and the TD-DFT excitation energies obtained for ***x*2** predict[53] a decrease in energy of the long-wave transition in the order **$^2$2** > **$^1$2** > **$^4$2** ≈ **$^6$2**, as was indeed observed (Table 3). Since **$^1$2** has the highest energy HOMO among *isomeric* ***x*2**, the conjugation effect, indeed, appears to be dominant in affecting the HOMO−LUMO separation upon −NC substitution of azulene. In addition, stabilization of the HOMO of **$^2$2** vs those of **$^4$2** and **$^6$2** is indicated, a fact not obvious from the qualitative considerations. This DFT prediction is nicely supported by the oxidation potential of **$^2$2** being 90 mV higher than that of **$^4$2** (Table 4). Electrochemical reduction and oxidation estimate the HOMO−LUMO gap for **$^2$2** to be somewhat wider than that for azulene (Table 4). While this result is consistent with the unexpected blue shift of azulene's $^1A \rightarrow {}^1L_b$ band upon −NC substitution at C-2, its significance is qualitative at best and should be taken with caution, because of irreversibility of the redox processes involved in the estimation.[54] Similarly, the redox properties of **$^4$2** are in accord with the red shift of **$^4$2**'s low-energy band relative to azulene. Notably, **$^4$2** and **$^6$2** exhibit fully reversible 1e$^-$ reductions (Table 4).

**Table 3. Comparison of Energies ($\lambda$ in nm, $\nu$ in cm$^{-1}$) of the Long-Wave Transitions for $^1$2, $^2$2, $^4$2, and $^6$2 vs Those for the Corresponding Cyanoazulenes**

| | $\lambda_{max}$ ($\nu_{max}$) | | |
|---|---|---|---|
| x | CN$^x$Az | NC$^x$Az | $\Delta\lambda_{max}$ ($\Delta\nu_{max}$)[a] |
| 1 | 589 (16 978)[b] | 558 (17 921)[b] | +31 (−943) |
| 2 | 565 (17 699)[b] | 586 (17 065)[c] | −21 (+634) |
| 4 | 603 (16 584)[b] | 628 (15 924)[d] | −25 (+660) |
| 6 | 609 (16 420)[b] | 631 (15 847)[e] | −22 (+573) |

[a] $\Delta\lambda_{max} = \lambda_{max}(CN^xAz) - \lambda_{max}(NC^xAz)$; $\Delta\nu_{max} = \nu_{max}(CN^xAz) - \nu_{max}(NC^xAz)$. [b] In pentane; this work. [c] In $C_6H_{12}$; ref 45. [d] In hexane; ref 46. [e] In $C_6H_{12}$; ref 47.

**Table 4. Oxidation and Reduction Potentials of Isocyanoazulenes vs FcH$^+$/FcH in $CH_2Cl_2$[a]**

| compd | $E_{p,c}$(red), V | $E_{p,a}$(ox), V | $E_{p,a}$(ox) − $E_{p,c}$(red) |
|---|---|---|---|
| azulene | −2.16 (i) | 0.54 (i) | 2.70 |
| **$^1$2** | −1.87 (i) | *d* | |
| **$^2$2** | −1.86 (i) | 0.92 (i) | 2.77 |
| **$^4$2** | −1.80 (r)[b] | 0.83 (i) | 2.61 |
| **$^6$2** | −1.79 (r)[c] | *d* | |

[a] Scan rate 100 mV/s; i = irreversible, r = reversible. [b] $E_{1/2}$ = −1.76 V, $i_{p,c}/i_{p,a}$ = 1.1, $\Delta E_{p,c-p,a}$ = 81 mV. [c] $E_{1/2}$ = −1.75 V, $i_{p,c}/i_{p,a}$ = 1.1, $\Delta E_{p,c-p,a}$ = 83 mV. [d] Not clearly defined.

**Scheme 1**

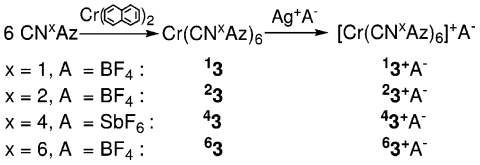


**Table 5. $E_{1/2}$ Potentials (in V) for $[Cr(CNR)_6]^{z/z+1}$ versus $[FcH]^0/[FcH]^+$ [a]**

| | R | | | | | |
|---|---|---|---|---|---|---|
| *z*/*z*+1 | $^1$Az | $^5$Az*[b] | Ph[c] | $^2$Az | $^6$Az | $^4$Az |
| 0/+ | −0.98 | −0.87 | −0.83 | −0.69 | −0.49 | −0.44 |
| +/+2 | −0.42 | −0.29 | −0.21 | −0.16 | −0.03 | +0.02 |

[a] All measurements were performed in $CH_2Cl_2/[^nBu_4N][PF_6]$ to ensure quantitative comparison, scan rate = 100 mV/s. [b] Az* = 1,3-di-*tert*-butylazulenyl. [c] Ref 57.

(51) The shifts are calculated from the UV−vis data reported in this work and in refs 24 and 45−48.

(52) For ***x*2** (and azulene derivatives in general), the $S_0 \rightarrow S_1$ excitation energies are significantly smaller than the corresponding HOMO−LUMO separations because of the electron correlation effect: Liu, R. S. H. *J. Chem. Educ.* **2002**, *79*, 183−185.

(53) While the differences in the excitation energies of ***x*2** are small, it is important to note that these azulenic systems are isomeric, and multiple approaches (TD-DFT, the B3LYP/6-31G(d,p) HOMO−LUMO gaps, and the HOMO−LUMO gaps of the MP2/6-31(d,p) optimized structures) gave the same trend.

(54) Conelly, N. G.; Geiger, W. *Chem. Rev.* **1996**, *96*, 877−910.

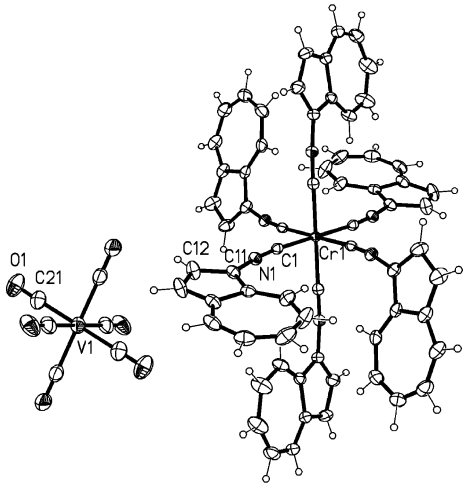


**Figure 7.** ORTEP (50%) diagram of $^{1}\mathbf{3}^{+}[V(CO)_6]$. Selected bond distances (Å) and angles (deg): Cr−C1 = 1.971(2), C1−N1 = 1.169(2), V−C21 = 1.952(2), C21−O1 = 1.153(3); C1−N1−C11 = 171.3(2).

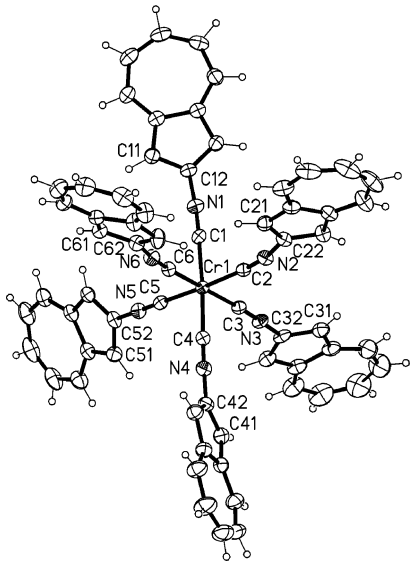


**Figure 8.** ORTEP (50%) diagram of $^{2}\mathbf{3}^{+}$. The $[BF_4]^-$ counterion is omitted for clarity. Selected bond distances (Å) and angles (deg): Cr−C1 = 1.973(3), Cr−C2 = 1.981(2), Cr−C3 = 1.972(3), Cr−C4 = 1.953(3), Cr−C5 = 2.001(3), Cr−C6 = 1.970(3), C1−N1 = 1.164(3), C2−N2 = 1.161(3), C3−N3 = 1.167(3), C4−N4 = 1.167(3), C5−N5 = 1.155(3), C6−N6 = 1.165(3); C1−N1−C12 = 175.4(3), C2−N2−C22 = 166.7(3), C3−N3−C32 = 172.5(3), C4−N4−C42 = 177.3(3), C5−N5−C52 = 174.9(2), C6−N6−C62 = 171.8(3).

The fine structures of the $S_0 \rightarrow S_1$ bands for $^{x}\mathbf{2}$ ($x$ = 1, 2, 4, 6) are virtually identical with those observed for the *corresponding* cyanoazulenes (e.g., Figure 3). Comparing energies of the long-wave transitions for $CN^{x}Az$ against those for the *corresponding* $NC^{x}Az$ should reflect difference in the inductive strengths of the isocyano vs cyano groups, all other factors being essentially equal, given the close structural relationship between the isomeric −NC and −CN fragments. Remarkably, the long-wave absorptions recorded for $^{2}\mathbf{2}$, $^{4}\mathbf{2}$, and $^{6}\mathbf{2}$ are all blue-shifted by very similar increments relative to 2-, 4-, and 6-cyanoazulenes, respectively (Table 3). This can be reasoned by less effective stabilization of the LUMO's of $^{2}\mathbf{2}$, $^{4}\mathbf{2}$, and $^{6}\mathbf{2}$ due to lower polarity of the isocyano group. On the other hand, the visible transition for $^{1}\mathbf{2}$ is red-shifted with respect to that for $NC^{1}Az$, reflecting the anticipated smaller inductive stabilization of $^{1}\mathbf{2}$'s HOMO.

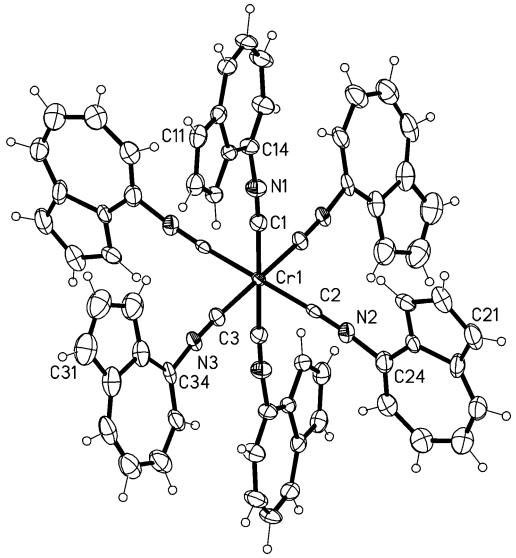


**Figure 9.** ORTEP (50%) diagram of $^{4}\mathbf{3}^{+}$ (major orientation). The $[SbF_6]^-$ counterion is omitted for clarity. The minor orientation of the ligands defined by C2 and C3 is shown in Figure S4 in the Supporting Information. Selected bond distances (Å) and angles (deg): Cr−C1 = 1.983(3), Cr−C2 = 1.964(4), Cr−C3 = 1.985(4), C1−N1 = 1.159(4), C2−N2 = 1.161(4), C3−N3 = 1.160(4); C1−N1−C14 = 175.7(4), C2−N2−C24 = 174.6(6), C3−N3−C34 = 175.2(7).

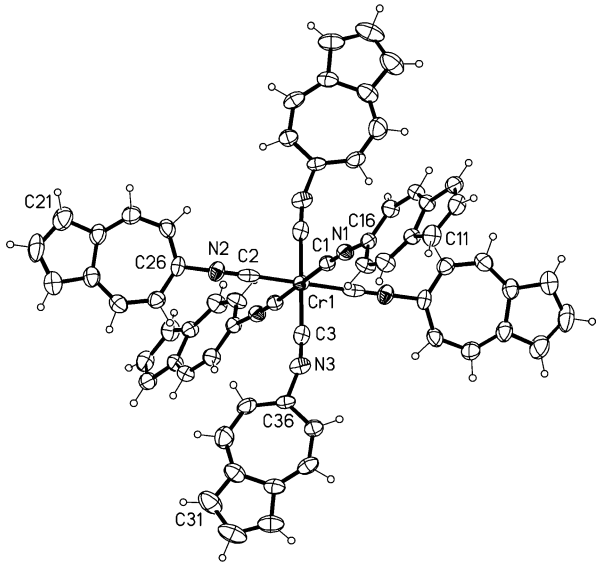


**Figure 10.** ORTEP (50%) diagram of $^{6}\mathbf{3}^{+}$. The $[BF_4]^-$ counterion is omitted for clarity. Selected bond distances (Å) and angles (deg): Cr−C1 = 1.946(7), Cr−C2 = 1.985(7), Cr−C3 = 1.974(7), C1−N1 = 1.188(7), C2−N2 = 1.176(7), C3−N3 = 1.175(7); average C1−N1−C16 = 175.8(6), C2−N2−C26 = 176.8(5), C3−N3−C36 = 160.4(6).

**Binary Complexes of $CN^{x}Az$: Probing Electronic Inhomogeneity of the Azulene Nucleus.** Compounds $^{x}\mathbf{2}$ ($x$ = 1, 2, 4, 6) react with $^{1}/_{6}$ equiv of $Cr(\eta^6\text{-naphthalene})_2$,[27] a highly labile analogue of $Cr(\eta^6\text{-}C_6H_6)_2$, to afford the corresponding thermally stable, octahedral complexes $Cr(\eta^1\text{-}CN^{x}Az)_6$ ($^{x}\mathbf{3}$) (Scheme 1). The complex $Cr(CN^{5}Az^{*})_6$ ($^{5}\mathbf{3}^{*}$) can be obtained from $^{5}\mathbf{2}^{*}$

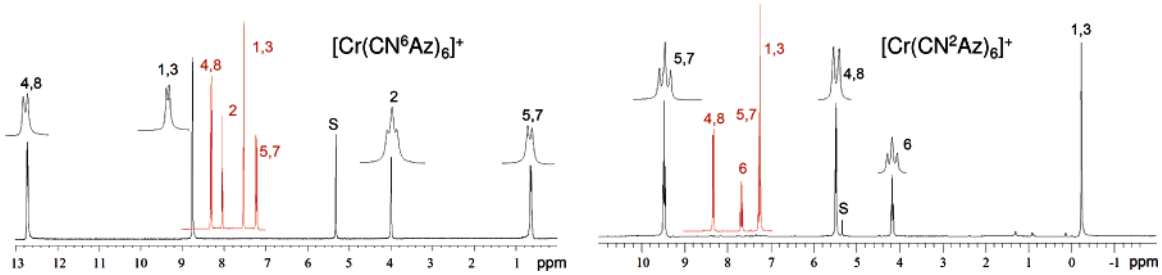


**Figure 11.** $^1$H NMR spectra of paramagnetic $^6$**3**$^+$[$BF_4$]$^-$ (left) and $^2$**3**$^+$[$BF_4$]$^-$ (right) in $CD_2Cl_2$ at 25 °C (S = solvent). The red inserts are the $^1$H NMR patterns of the corresponding diamagnetic $^6$**2** and $^2$**2** recorded under the same conditions.

in an analogous manner.[55] Such a mode of reactivity is particularly remarkable in the case of $^1$**2**, given that its LUMO is entirely azulene-based (Figure 6), while the lone pair of the terminal carbon atom is involved only in the HOMO-2. While $^1$**3** and $^4$**3** readily dissolve in polar organic solvents, $^2$**3** and $^6$**3** are practically insoluble in THF, $CH_2Cl_2$, $CHCl_3$, and $CH_3CN$. We attribute the poor solubility of $^2$**3** and $^6$**3** to extensive intermolecular $\pi$-stacking interactions between the radially oriented $^2$-Az or $^6$Az groups (vide infra). Upon treatment with $Ag^+$, all $^x$**3** species undergo oxidation to form the corresponding paramagnetic cations $^x$**3**$^+$ (Scheme 1). Unlike their neutral precursors, $^2$**3**$^+$[$BF_4$]$^-$ and $^6$**3**$^+$[$BF_4$]$^-$ are quite soluble in polar organic solvents. The energies of the "$T_{1u}$"-like $\nu_{CN}$ bands for $^x$**3** (1950−1954 $cm^{-1}$) and $^x$**3**$^+$ (2034−2053 $cm^{-1}$) are depressed with respect to those of $^x$**2** (Table 2), indicating substantial back-bonding in $^x$**3** and $^x$**3**$^+$. The low-spin $d^5$ formulation of $^x$**3**$^+$ ($x$ = 1, 2, 4, 6) is in accord with their $\mu_{eff}$ values of 1.71−2.07 $\mu_B$ at 25 °C.

Whereas $^1$**3** is readily oxidized by $V(CO)_6$ to afford $^1$**3**$^+$[$V(CO)_6$]$^-$, $^4$**3** and $^6$**3** are practically unaffected by this mild 17-electron oxidizing agent. Combining $^2$**3** with $V(CO)_6$ produces an equilibrium mixture of $^2$**3**, $V(CO)_6$, and $^2$**3**$^+$[$V(CO)_6$]$^-$. Thus, changing the atom of attachment of the Az groups substantially alters the electron richness of the "$Cr(CN)_6$" core. The half-wave potentials for the quasi-reversible, Cr-centered redox processes $[Cr(CNR)_6]^{z/z+1}$ ($z$ = 0, 1) are listed in Table 5. These data imply that the $\sigma$-donor/$\pi$-acceptor ratio[56] of the isocyanide ligands decreases in the order $CN^1$Az < $CN^5$-Az < CNPh < $CN^2$Az < $CN^6$Az < $CN^4$Az.

Remarkably, the difference between the first oxidation potentials of *isomeric* $^1$**3** and $^4$**3** exceeds 0.5 V and $E_{1/2}([Cr(CN^1Az)_6]^{+/2+}) \approx E_{1/2}([Cr(CN^4Az)_6]^{0/+})$. This makes the Cr(I) center in $^1$**3**$^+$ as electron-rich as Cr(0) in $^4$**3**. Such a dramatic difference in the oxidation potentials of $^1$**3** and $^4$**3** is a direct consequence of electronic inhomogeneity of the azulenyl substituents. The $E_{1/2}$ potential of the $[Cr(CN^1Az)_6]^{0/+}$couple is virtually equal to that of $[Cr(CNFc)_6]^{0/+}$ (−0.97 V),[18a] suggesting identical donor/acceptor characteristics of the $CN^1$Az and CNFc ligands. The "electrochemical series" in Table 5 constitutes a quantitative measure of electronic inhomogeneity of the azulenic framework and correlates nicely with the trend of p$K_a$ values measured for azuloic acids: 6.99 (HO(O)$C^1$Az) > 5.86 (HO(O)$C^2$Az) > 5.21 (HO(O)$C^6$Az).[58] However, HO(O)$C^4$Az remains unknown, and quantitative interpretation of its acidity would likely be compromised by expected intramolecular hydrogen bonding between the oxygen of the carbonyl group and the H atom at position 1 of the azulenic nucleus.[58]

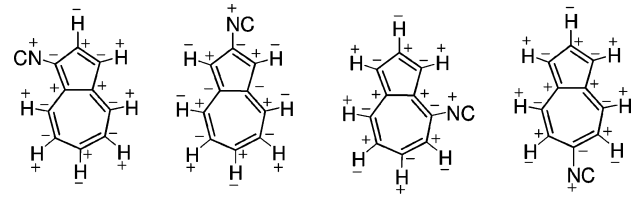

**Figure 12.** From left to right: observed directions of the $^1$H, $^{13}$C, and $^{14}$N paramagnetic shifts for the nuclei in $^1$**3**$^+$, $^2$**3**$^+$, $^4$**3**$^+$, and $^6$**3**$^+$. The symbols "−" and "+" denote upfield and downfield shifts, respectively, relative to chemical shifts of the nuclei in the corresponding diamagnetic $^x$**2**.

The X-ray structures of $^1$**3**$^+$, $^2$**3**$^+$, $^4$**3**$^+$, and $^6$**3**$^+$ are illustrated in Figures 7−10, respectively. The metric parameters of $^1$**3**$^+$[$V(CO)_6$]$^-$ (Figure 7), both the cation and anion of which exhibit only one crystallographically independent ligand, are fully in accord with the electron transfer from $^1$**3** to $V(CO)_6$ that occurs upon mixing the two electroneutral complexes. The V−C bond lengths of 1.952(2) Å in the $[V(CO)_6]^-$ anion compare well with the V−C distances found for several other salts of $[V(CO)_6]^-$ [18a,59] and are statistically shorter than those reported for neutral $V(CO)_6$ (1.993(2), 2.005(2) Å).[60] At the same time, the C−O bonds in $^1$**3**$^+$[$V(CO)_6$]$^-$ (1.153(3) Å) are longer than those determined for $V(CO)_6$ (1.123(2), 1.136(3) Å).[60]

Each of the isomeric cations $^x$**3**$^+$ (Figures 7−10) features six discrete azulenyl groups bound to the nearly octahedral $Cr(CN)_6$ cores. The Cr−C and C−N$^x$Az bond lengths and C−N−C angles are very similar for all $^x$**3**$^+$ and are also comparable to the corresponding parameters observed for $[Cr(CNFc)_6]^+$ [18a] and $[Cr(CNPh)_6]^+$ [61] (Table 6). As in azulene,[62] the peripheral C−C distances

(55) Deep purple $Cr(CN^5Az^*)_6$ ($^5$**3***) was prepared by treating Cr($\eta^6$-naphthalene)$_2$ with 6 equiv of $^5$**2*** in THF at 20 °C followed by removing all volatiles (including free naphthalene) at $10^{-2}$ Torr. IR ($CH_2Cl_2$): $\nu_{CN}$ 1953 vs br $cm^{-1}$.

(56) Treichel, P. M. *Adv. Organomet. Chem.* **1973**, *11*, 21−86.

(57) (a) Bullock, J. P.; Mann, K. R. *Inorg. Chem.* **1989**, *28*, 4006−4011. (b) Treichel, P. M.; Essenmacher, G. J. *Inorg. Chem.* **1976**, *15*, 146−150.

(58) McDonald, R. N.; Reitz, R. R. *J. Org. Chem.* **1972**, *37*, 2703−2705.

(59) (a) Doyle, G.; Eriksen, K. A.; Van Engen, D. *Organometallics* **1985**, *4*, 2201−2206. (b) Calderazzo, F.; Pampaloni, G.; Lanfranchi, M.; Pelizzi, G. *J. Organomet. Chem.* **1985**, *296*, 1−13. (c) Calderazzo, F.; Pampaloni, G.; Vitali, D.; Zanazzi, P. F. *J. Chem. Soc., Dalton Trans.* **1982**, 1993−1997. (d) Silverman, L. D.; Corfield, P. W. R.; Lippard, S. J. *Inorg. Chem.* **1981**, *20*, 3106−3109. (e) Wilson, R. D.; Bau, R. *J. Am. Chem. Soc.* **1974**, *96*, 7601−7602.

(60) Bellard, S.; Rubinson, K. A.; Sheldrick, G. M. *Acta Crystallogr.* **1979**, *B47*, 271−274.

(61) Bohling, D. A.; Mann, K. R. *Inorg. Chem.* **1984**, *23*, 1426−1432.

(62) Hanson, A. W. *Acta Crystallogr.* **1965**, *19*, 19−26.

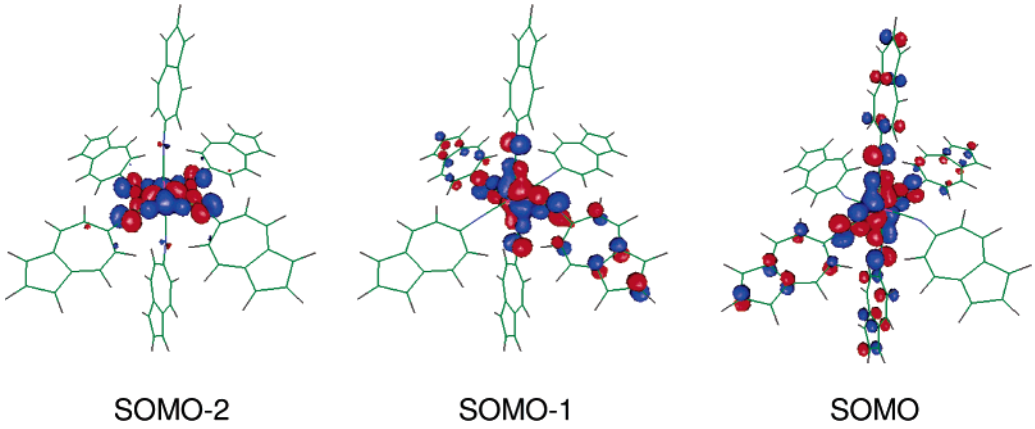


**Figure 13.** The nearly degenerate set of the highest occupied MO's of $^{6}\mathbf{3}^{+}$ (solid-state structure, SOMO = singly occupied molecular orbital; $[BF_4]^-$ counterion is omitted for clarity).

**Table 6. Selected Average Metric Parameters for $^{x}\mathbf{3}^{+}$ ($x$ = 1, 2, 4, 6)[a]**

| | Cr−C, Å | C−NAz, Å | C−N−C, deg |
|---|---|---|---|
| $^{1}\mathbf{3}^{+}$ | 1.971(2) | 1.169(2) | 171.3(2) |
| $^{2}\mathbf{3}^{+}$ | 1.97(2) | 1.163(5) | 173(4) |
| $^{4}\mathbf{3}^{+}$ | 1.98(3) | 1.160(4) | 175(1) |
| $^{6}\mathbf{3}^{+}$ | 1.97(2) | 1.179(8) | 171(9) |
| $[Cr(CNFc)_6]^{+}$ [b] | 1.97(2) | 1.160(3) | 171(4) |
| $[Cr(CNPh)_6]^{+}$ [c] | 1.97(2) | 1.158(6) | 177(2) |

[a] Numbers in parentheses constitute the standard deviations of the mean. [b] Reference 18a. [c] Reference 61.

within the azulenyl groups in $^{x}\mathbf{3}^{+}$ do not show appreciable alternation and are ca. 0.1 Å shorter than the C−C bonds at the ring junctions. The cations $^{1}\mathbf{3}^{+}$ and $^{4}\mathbf{3}^{+}$ exhibit intermolecular $\pi$-stacking interactions between azulenyl groups (Figures S1 and S3 in the Supporting Information). The interacting azulenyl moieties are aligned in an antiparallel fashion (cf. *anti*-azulenophanes[63]), with interplanar separations being 3.313(7) and 3.29(5) Å for $^{1}\mathbf{3}^{+}$ and $^{4}\mathbf{3}^{+}$, respectively. Such a packing mode minimizes electrostatic interactions between the azulenic pairs involved in $\pi$-stacking and was also suggested to occur in certain azulene-based liquid crystals.[10b] The cations $^{2}\mathbf{3}^{+}$ are involved in offset face-to-face intermolecular $\pi$-stacking interactions between azulenic five-membered rings with interplanar separations of 3.44(2) Å (Figure S2 in the Supporting Information).

Owing to their degenerate ideal $^{2}$T ground states, the paramagnetic cations $^{x}\mathbf{3}^{+}$ ($x$ = 1, 2, 4, 6) exhibit short relaxation times $T_{1e}$[64] and give narrow $^{1}$H, $^{13}$C, and $^{14}$N NMR signals (e.g., Figure 11). The $^{1}$H paramagnetic shifts observed for all $^{x}\mathbf{3}^{+}$ are practically contact in origin because of the high symmetry of the complexes (small Jahn−Teller distortions possible for these cations are dynamic on the NMR time scale) and occur in both directions, suggesting the presence of unpaired spin in the $\pi$-systems of the azulenyl groups.[64,65] Indeed, the paramagnetic shifts of $^{1}$H and the corresponding $^{13}$C resonances for $^{x}\mathbf{3}^{+}$ occur in opposite directions, and the $^{13}$C paramagnetic shifts alternate their sign throughout *peripheries* of the azulenyl moieties, as summarized in Figure 12.[66] To the best of our knowledge, $^{x}\mathbf{3}^{+}$ ($x$ = 1, 2, 3, 6) represent the only azulenic $\pi$-systems for which unpaired spin delocalization has been observed by NMR.

Examination of the frontier molecular orbitals of $^{6}\mathbf{3}^{+}$- and $^{1}\mathbf{3}^{+}$ by DFT indicated that the Cr(d$\pi$)→CN$^{x}$Az(p$\pi$*) interaction is an important (but not necessarily sole[18a,65]) contributor to the mechanism of unpaired spin delocalization in these low-spin d$^5$ complexes. For example, Figure 13 clearly implies delocalization of unpaired electron into *both* rings of the azulenyl groups in $^{6}\mathbf{3}^{+}$ by means of back-bonding.[67] Such a mechanism places unpaired spin into the p orbitals of C$^2$, C$^{5,7}$, and the atoms at the ring junctions of the $^{6}$Az groups. Consequently, the $^{13}$C resonances for these nuclei undergo downfield paramagnetic shifts (relative to the corresponding resonances for diamagnetic $^{6}\mathbf{2}$), while the $^{13}$C peaks for the remaining carbon atoms of the $^{6}$Az substituents exhibit upfield paramagnetic shifts owing to spin polarization[64] of the azulenic $\pi$-systems (Figure 12, right). The atomic exchange coupling[64] polarizes (i.e., unpairs) electrons of the C(sp$^2$)−H bonds, resulting in upfield paramagnetic shifts of the $^{1}$H resonances for the H$^2$ and H$^{5,7}$ nuclei and downfield paramagnetic shifts of the $^{1}$H peaks for the H$^{4,8}$ and H$^{1,3}$ nuclei (Figure 11, left).

## Concluding Remarks

The five possible isocyanoazulenes, the four archetypal species CN$^{x}$Az ($x$ = 1, 2, 4, 6) and the 1,3-di-*tert*-butyl derivative of CN$^5$Az, were efficiently synthesized and isolated on a practical scale. Unlike many of their benzenoid congeners, these highly colored isocyanides exhibit good thermal stability, low sensitivity to air, and have relatively mild or practically no odor. Considering the potent electron-withdrawing nature of the isocyano group, CN$^1$Az and CN$^2$Az show "anomalous" shifts of the $S_0 \rightarrow S_1$ transition relative to azulene. These phenomena were rationalized by means of the DFT calculations, cyclic voltammetry, and comparison of the electronic spectra of CN$^{x}$Az with those of the corresponding cyanoazulenes.

(63) (a) Koenig, T.; Rudolf, K.; Chadwick, R.; Geiselmann, H.; Patapoff, T.; Klopfenstein, C. E. *J. Am. Chem. Soc.* **1986**, *108*, 5024−5025. (b) Luhowy, R.; Keehn, P. M. *J. Am. Chem. Soc.* **1977**, *99*, 3797−3805.

(64) LaMar, G. N., Horrocks, W. D., Jr., Holm, R. H., Eds. *NMR of Paramagnetic Molecules*; Academic Press: New York, 1973.

(65) Barybin, M. V.; Young, V. G., Jr.; Ellis, J. E. *J. Am. Chem. Soc.* **2000**, *122*, 4678−4691.

(66) Detailed analysis of the NMR patterns for $^{x}\mathbf{3}^{+}$ will be reported elsewhere: Barybin, M. V.; Holovics, T. C. Manuscript in preparation.

(67) See Figure S11 in the Supporting Information for the analogous analysis of $^{1}\mathbf{3}^{+}$.

Despite the high propensity of the azulenic nucleus to undergo multihapto coordination to low-valent metals, six azulenic moieties were electronically coupled to the Cr(0) and Cr(I) centers via conducting isocyanide linkers. Changing the position of attachment of the azulenyl groups to the "$Cr(CN)_6$" core in $[Cr(CN^xAz)_6]^z$ substantially altered the donor/acceptor ratio of the isocyanoazulene ligands and provided a unique approach for quantitative electrochemical assessment of electronic inhomogeneity of the azulenic framework. The species $CN^4Az$ and $CN^6Az$ have the lowest donor/acceptor ratios among hydrocarbon-substituted isocyanides known. For the first time, unpaired spin delocalization within the azulenic $\pi$-systems was observed by NMR. The $Cr^I(d\pi) \rightarrow CN^xAz(p\pi^*)$ interaction has been shown to be an important contributor to the mechanism of unpaired electron delocalization within $[Cr(CN^xAz)_6]^+$. Given the relatively small aromatic stabilization energy of azulene[49] and compatibility of $CN^xAz$ with low-valent metals, diisocyanoazulenes (2,6-diisocyanoazulene in particular) are attractive for designing electron-rich organometallic supramolecular ensembles incorporating a bridging azulenic moiety. Work toward such systems is in progress in our laboratory.

**Acknowledgment.** Financial support of this work was provided by the Kansas NSF EPSCoR, Kansas Technology Enterprise Corp., and the University of Kansas. M.V.B. thanks the KU Center for Research for the New Faculty GRF Award.

**Supporting Information Available:** Complete description of the X-ray crystallographic work for $^1\mathbf{3}^+[V(CO)_6]^-$, $^2\mathbf{3}^+[BF_4]^-$, $^4\mathbf{3}^+[SbF_6]^-$, and $^6\mathbf{3}^+[BF_4]^-$, details of electrochemical experiments and cyclic voltammograms of $^1\mathbf{3}$, $^2\mathbf{3}^+[BF_4]^-$, $^4\mathbf{3}$, $^5\mathbf{3}^*$, and $^6\mathbf{3}^+[BF_4]^-$, details of DFT calculations, and complete references 31 and 34. This material is available free of charge via the Internet at http://pubs.acs.org.

OM0502180